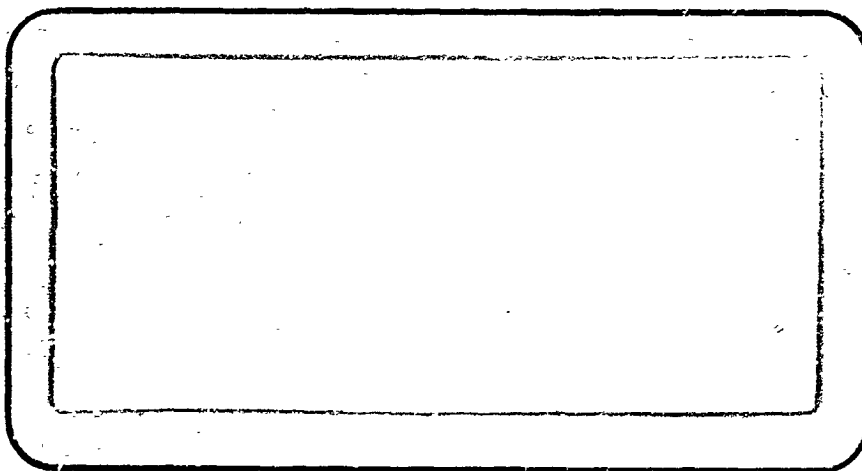


~~AD~~/COM I



N65-24994

(ACCESSION NUMBER)

59

(PAGES)

CD 62963

(NASA UR OR TMX OR AD NUMBER)

(THRU)

1

(CODE)

09

(CATEGORY)

GPO PRICE \$ _____

OTS PRICE(S) \$ _____

Hard copy (HC) 3.00

Microfiche (MF) .50

ADCOM, INC.
808 Memorial Drive
Cambridge 39, Mass.
UN 8-7386

**Second Quarterly Report
ADVANCED THRESHOLD REDUCTION
TECHNIQUES STUDY**

1 October 1964 - 31 December 1964

Contract No. NAS 5-9011

**Prepared for
National Aeronautics and Space Administration
Goddard Space Flight Center
Greenbelt, Maryland**

**by
ADCOM, Inc.
808 Memorial Drive
Cambridge, Massachusetts**

Second Quarterly Report

ADVANCED THRESHOLD REDUCTION
TECHNIQUES STUDY

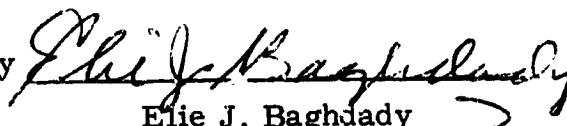
(1 October 1964 - 31 December 1964)

Contract No. NAS 5-9011

Prepared for

National Aeronautics and Space Administration
Goddard Space Flight Center
Greenbelt, Maryland

Approved by



Elie J. Baghdady
Technical Director

ADCOM, Inc.
808 Memorial Drive
Cambridge, Massachusetts

TABLE OF CONTENTS

<u>Section</u>		<u>Page</u>
I	GENERAL INTRODUCTION	1
II	SYNOPSIS OF RESULTS	3
III	ANALYTICAL STORY OF BAND-DIVIDING DEMODULATION TECHNIQUES	5
	3.1 Introduction	5
	3.2 PLL Band-Dividing	6
	3.3 Band-Dividing Demodulation: Signal Estimation Techniques	12
	3.3.1 A Maximum Likelihood Band-Dividing FM Demodulator	12
	3.3.1.1 Signal and Noise Characterization	12
	3.3.1.2 Signal Estimation	16
	3.3.2 A Simple Interpolation Scheme	22
	3.3.3 Effect of Mis-Selection Noise in Systems with Filter Overlap.	24
IV	EXPERIMENTAL RESULTS	29
	4.1 The Automatic Threshold Curve Plotter	29
	4.2 The Second Order PLL	31
V	HIGHER ORDER PLL DESIGN	41
	5.1 The Third Order PLL	41
	5.2 The Optimum Realizable PLL: Case of a Rectangular Spectrum	43
	5.2.1 Determination of the Closed Loop Transfer Function	43
	5.2.2 Determination of the Open Loop Transfer Function	48
VI	OUTLINE OF WORK PLANS	55
	6.1 Theoretical Work.	55
	6.2 Experimental Work	55

LIST OF ILLUSTRATIONS

<u>Figure</u>		<u>Page</u>
1	$\omega_2 - \omega_1 \ll \Omega_{\text{pull-in}}$	7
2	$\omega_2 - \omega_1 \sim \Omega_{\text{pull-in}}$	7
3	$\omega_2 - \omega_1 \sim \Omega_{\text{pull-in}}, \omega_2 \omega_o > \Omega_{\text{pull-in}}$	8
4	Frequency pull-in time of a second-order phase-locked loop. The dotted lines characterize the pull-in ranges for the different $m = \tau_1/\tau_2$	10
5	Block diagram of maximum likelihood estimator (case of no-memory processing)	21
6	Contours of $P'_{n2}/P_{n2} = 1$, for various N	27
7	Block diagram of automatic test system	30
8	Block diagram of second order PLL	32
9	Schematic of PLL	33
10	VCO linearity	34
11	VCO amplitude vs. frequency	35
12	Second order PLL performance for $\delta = 30$	37
13	Second order PLL performance for $\delta = 20$	38
14	Second order PLL performance for $\delta = 10$	39
15	Threshold curve for third order loop filters	47
16	Configuration of active filter network	50
17	Circuits for synthesizing impedances	52

LIST OF TABLES

<u>Table</u>		<u>Page</u>
I	LOOP PARAMETERS AT THRESHOLD	46
II	TIME CONSTANT VALUES	49
III	COMPONENT VALUES FOR $Z(s)$	51
IV	COMPONENT VALUES FOR $Z'(s)$	53

I. GENERAL INTRODUCTION

This document constitutes the Second Quarterly Progress Report submitted by ADCOM, Inc. to the NASA Goddard Space Flight Center under Contract No. NAS5-9011. The work covered here was performed at ADCOM, Inc. between 1 October 1964 and 31 December 1964.

The primary objective of this program is to demonstrate the feasibility of reducing the noise threshold for demodulating FM signals at least 3 db below the threshold experienced with a second order PLL demodulator whose design is optimized for best threshold performance in demodulating a given signal.

The previous effort on the program has been concentrated on the evaluation of the current state of knowledge of the most promising threshold reduction techniques and on the analytical study of some of these promising techniques, as well as on the design and instrumentation of the experimental test set-up. This report presents the logical continuation of these efforts. On this basis:

Section II of this report presents a synopsis of the results and conclusions reported in the main body of the report.

Section III presents and evaluates the performance of several band-dividing techniques motivated by some of the limitations found in the original work of Akima.

Section IV presents the experimental effort on the program which consists of the completion of the automatic test system and the implementation and tests of second order loops.

✓Section V discusses the synthesis of higher order PLL demodulators.

Section VI finally outlines the work plans for the next interval.

II. SYNOPSIS OF RESULTS

The present section summarizes the results and conclusions of the sections that follow.

Section III is concerned with the study of several band-dividing techniques. Each filter of the original band-dividing bank proposed by Akima requires a minimum bandwidth from transient response considerations. This minimum bandwidth limits the ratio B_f/B_{if} of the individual filter to the i-f bandwidths, and hence limits the number of filters and the achievable threshold improvement of the Akima (non-overlapping) filters. Moreover, the filter bandwidth B_f has the same functional dependence on the modulation index and frequency as a second order PLL demodulator, and comparable coefficients, so that the improvement capabilities of the Akima system, even in the absence of mis-selection effects, are expected to be inferior to those attainable by the PLL demodulator in question.

A possible approach to overcome this difficulty is to have a filter bandwidth narrower than that required to capture the signal, an idea which suggests the study of a PLL band-dividing bank where each i-f division is the pull-in range of a loop. The system constraint is that

$$\text{max rate of frequency change} \times \text{acquisition time} \ll \text{pull-in range}$$

and the analytical study of this condition shows that the bandwidth required for each PLL in order to satisfy this constraint is so large that the performance is inferior to a second order PLL demodulator.

On this basis, we turn our attention to schemes that do not rely on the ratio B_f/B_{if} for threshold improvement, i. e., where the output FM signal is not obtained through some sort of discriminator operation but is treated as a signal parameter estimation problem. A maximum likelihood FM demodulator

that processes the output of a band-dividing filter bank is characterized for the case of no-memory processing. This estimator can only be simplified when the filter outputs do not overlap but in this case the transient response constraint will yield a small number of filters that span the whole i-f. A simpler signal estimator technique based on an interpolation of the outputs of three filters is described.

Finally, the effects of mis-selection noise are studied by substituting the simple case of Akima by another one where a large amount of overlap is assumed for the two adjacent filters relative to the other ones that are further apart. The two cases are then compared on the basis of their mis-selection noise performance.

Section IV describes the experimental effort. The automatic threshold curve plotter has been successfully completed and its operation is summarized. The second order PLL is also presented and particular attention is given to the loop filter design in accordance with the optimization discussed in the previous report. These PLL's have been implemented for modulation indices of 10, 20, 30 and some sample threshold curves that compare their performance to that of a conventional FM demodulator are obtained with the automatic test system. The large index improvement capabilities of the PLL is clearly indicated, as well as the disappearance of this improvement as the index is reduced. The theoretical logic behind these results is explained and the use of higher order loops is motivated.

Section V presents the design of higher order loop filters for the cases of sinusoidal and rectangular-spectrum modulating signals. The third order loop optimization for sinusoidal modulation is presented and two alternate filter designs are given. Also, the optimum realizable PLL transfer function for the case of a rectangular message spectrum is approximated by a third order filter and properly modified to yield a d-c path in the loop. Once the loop filter transfer function is found, its synthesis by an active RC network is discussed and design parameters are given.

III. ANALYTICAL STORY OF BAND-DIVIDING DEMODULATION TECHNIQUES

3.1 Introduction

The band-dividing system of Akima¹ shows a SNR improvement over conventional FM demodulation. This improvement is based on the use of a smaller predetection bandwidth than that required in conventional FM which is obtained by dividing the predetection i-f by means of a filter bank, identifying the presence of a signal in one of the filters and demodulating the individual filter output in a conventional way. If the correct filter is always selected, then the SNR (and threshold) improvement is given by B_{if}/B_f , where B_f is the filter bandwidth. The presence of noise causes incorrect filter selection thus reducing the improvement capabilities.

The filter bandwidth constraints for a CW sinusoidal modulation were evaluated in the First Quarterly Report² from transient response considerations and it was shown that this bandwidth was of the same order of magnitude of the conventional second order PLL demodulator optimized for this modulation. This result is independent of the degree of filter overlap and of mis-selection noise considerations. It states that based only on the signal tracking requirement, the SNR (and threshold) improvement of the Akima system is comparable to that of the second order PLL. When mis-selection noise is also considered, then the band-dividing performance would be worse and this seems sufficient evidence to direct our approach toward other solutions.

In particular, it should be noted that these results will be applicable to any band-dividing scheme based on a filter bank followed by conventional FM demodulation, i. e., where the SNR improvement is given by B_{if}/B_f for high SNR. The actual filter selection scheme can only alter the mis-selection noise performance, i. e., the extent to which the maximum improvement of B_{if}/B_f is approximated.

In analogy with the passive filter bank, a necessary condition for the signal reproduction is that the signal frequency variation during the acquisition time remains within the pull-in range of the loop in question. In general, one can distinguish between two acquisition modes for a signal with arbitrary phase dynamics. The first case consists of the semi-instantaneous acquisition of the signal so that the difference between the signal frequency at $t = 0$ and at $t = t_{acq}$ is very small relative to the pull-in range, as shown in Fig. 1. This case may be treated analytically as the acquisition of a constant frequency step

$$\Omega \approx \omega_0 - \omega_1 \approx \omega_0 - \omega_2. \quad (3.1)$$

Notice that even in the case where

$$|\omega_1 - \omega_0| > \Omega_{\text{pull-in}}$$

and

$$|\omega_2 - \omega_0| > \Omega_{\text{pull-in}}$$

* The pull-in range of a PLL is defined as the maximum constant frequency step, referred to the free running VCO, that can be required.

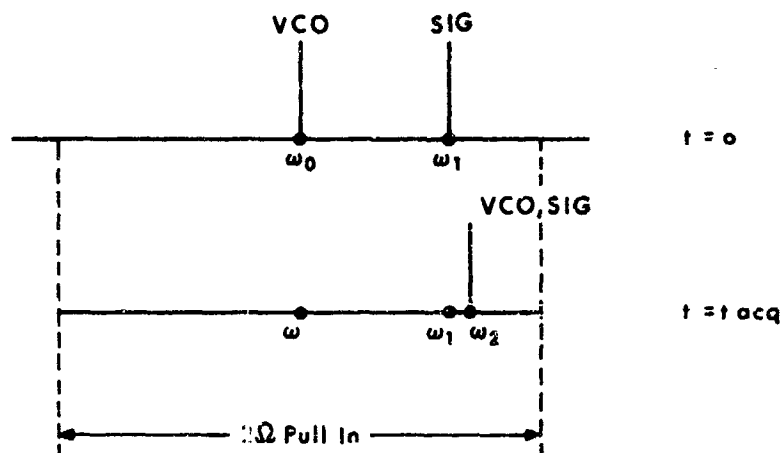


Fig. 1 $\omega_2 - \omega_1 \ll \Omega_{\text{pull-in}}$.

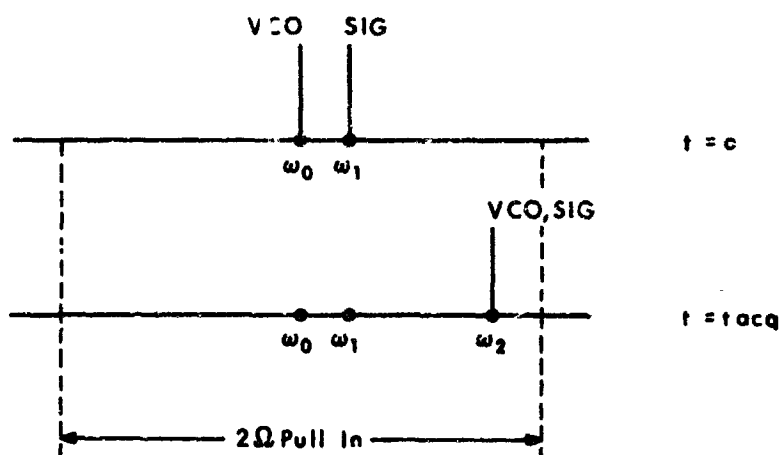


Fig. 2 $\omega_2 - \omega_1 \sim \Omega_{\text{pull-in}}$.

the analysis makes sense since it is just a question of whether a given loop or its adjacent one acquires the signal. The second case consists of the alternate possibility where the difference between the signal frequency at $t = 0$ and t_{acq} is comparable to the pull-in range, as shown in Fig. 2. The analysis in this case must include the actual phase fluctuations formulation and it becomes very complicated due to the nonlinearities involved in the acquisition process. Still, one can note an undesirable feature in this case. Consider the possibility of

$$|\omega_1 - \omega_0| < \Omega_{\text{pull-in}}$$

and

$$|\omega_2 - \omega_0| > \Omega_{\text{pull-in}}$$

which should happen rather frequently for the case in question and is characterized in Fig. 3. It is noted that even if the adjacent loop were to acquire, which is not certain, the signal is lost during the transition time to the adjacent loop.

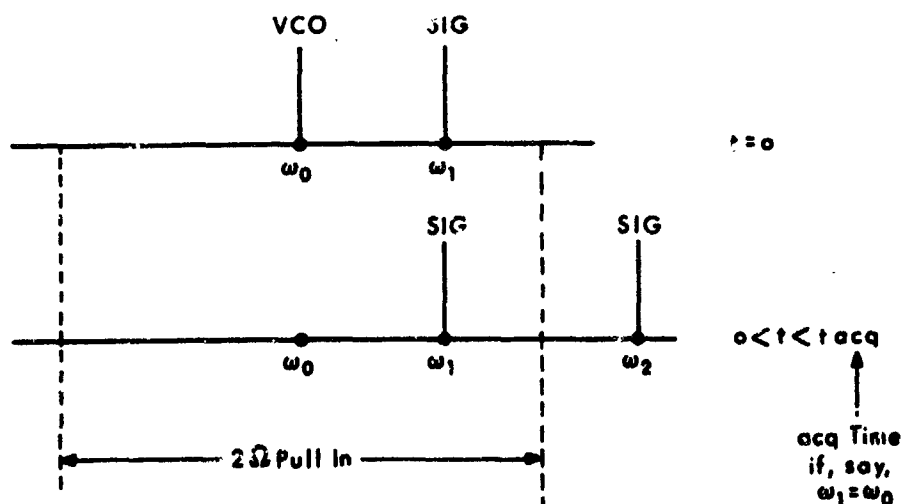


Fig. 3 $\omega_2 - \omega_1 \sim \Omega_{\text{pull-in}}$, $|\omega_2 - \omega_0| > \Omega_{\text{pull-in}}$

This phenomenon was not relevant in the first case since these transitions do not occur frequently because acquisition takes place before the signal has moved away, and whenever they occur, the transition time is of the order of the acquisition time. It is evident that the second acquisition mode seems undesirable from reliability considerations and that the first mode is thus desired. The acquisition requirement for sinusoidal modulation is then

$$\begin{array}{ccccc} \text{max rate of} & \times & \text{acquisition} & << & \text{pull-in} \\ \text{freq change} & & \text{time} & & \text{range} \\ (\delta \omega_m^2) & & (t_{\text{acq}}) & & (\Omega_{\text{pull-in}}) \end{array}$$

The analysis that follows assumes a conventional second order loop having the set (K, B_n, a) as design parameters.² The acquisition time of a frequency step by such a system may be approximated by

$$\Omega^2 / a(2-a)^2 B_n^3, \quad (3.2)$$

where Ω is the initial frequency shift in rad/sec, as long as Ω is sufficiently smaller than the pull-in range. A more detailed plot of the acquisition time is shown in Fig. 4. in terms of (K, τ_1, τ_2) and is based on the analytical work of Richman³. (The acquisition time results of Viterbi⁴ are but a special case of these curves.) As Ω gets closer to the pull-in range, the actual acquisition time becomes increasingly larger than that given by the previous expression and finally $t_{\text{acq}} = \infty$ for $\Omega = \Omega_{\text{pull-in}}$. Therefore,

$$\delta \omega_m^2 \times \frac{\Omega^2}{a(2-a)^2 B_n^3} << \Omega_{\text{pull-in}}^{\text{suff}} \text{ for } \Omega < \Omega_{\text{pull-in}}. \quad (3.3)$$

The worst case for acquisition occurs at $\Omega = \Omega_{\text{pull-in}}$. Even though the previous formulation is not valid at this value, it is still of interest to use $\Omega = \Omega_{\text{pull-in}}$ because if an undesirable performance results, as will be the case, one can then claim that the actual performance is even worse and conclude that the system is inferior to other techniques.

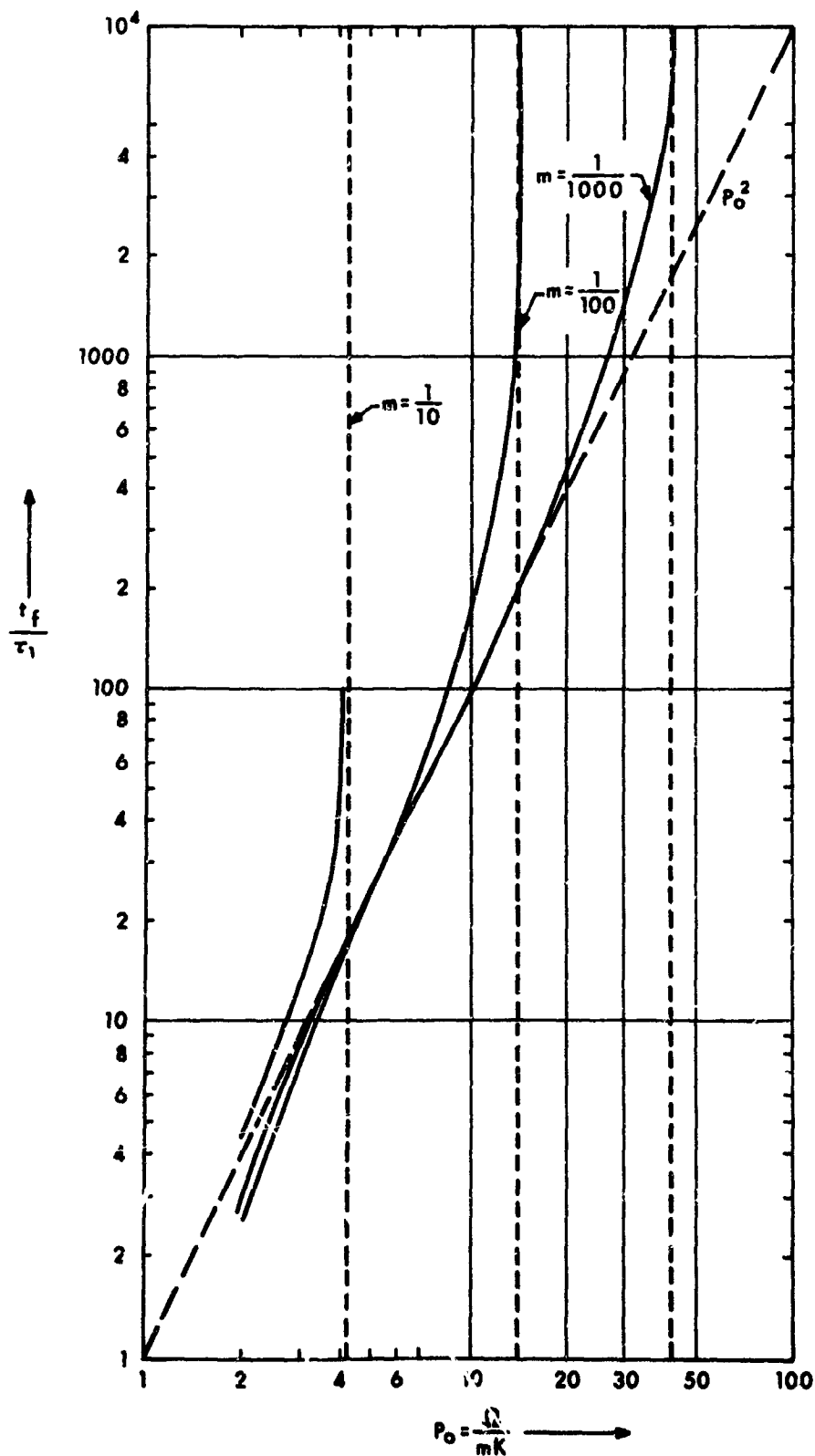


Fig. 4 Frequency pull-in time of a second order phase-locked loop. The dotted lines characterize the pull-in ranges for the different $m = \tau_1/\tau_2$.

The pull-in range of the second order loop in question is given by^{5*}

$$\Omega_{\text{pull-in}} \approx \sqrt{2(2-a) B_n K} \quad (3.4)$$

so that the acquisition requirement reads

$$B_n^{5/2} \gg \frac{\sqrt{2K}}{2(2-a)^{3/2}} \delta \omega_m^2 \quad (3.5)$$

so that using a factor of 10 to account for the much greater sign and setting $a = 1$ which gives a near-optimum behavior, then

$$B_n > 1.2 \left(\frac{K}{B_n} \right)^{1/4} \sqrt{\delta} \omega_m \text{ cps.} \quad (3.6)$$

A comparison with the optimized second order PLL demodulator² shows that each PLL in the bank requires a noise bandwidth equal to or larger than that of a single PLL processing the whole i-f signal since $K \gg B_n$. Notice that the K parameter for the PLL bank is established from the steady-state error $\phi = \Omega/K$ so that using $\phi < \frac{1}{2}$ radian (certainly an upper bound), for instance,

$$K > \frac{\Omega}{\phi} = \frac{1}{\phi} \sqrt{2B_n K} \quad \text{for } \Omega = \Omega_{\text{pull-in}}, a = 1 \quad (3.7)$$

or

$$\left(\frac{K}{B_n} \right)^{1/4} > \frac{1.2}{\sqrt{\phi}} > 1.7 \quad (3.8)$$

so that

$$B_n > 2 \sqrt{\delta} \omega_m \text{ cps} \quad (3.9)$$

which is comparable to the noise bandwidth of the single PLL demodulator.

This result seems to be sufficient evidence to discard the conventional PLL band-dividing scheme, particularly if the aforesaid correction for the acquisition time is accounted for. This statement must be revised if faster acquisition capabilities are included, such as VCO sweeps (which is probably undesired because of the on-off synchronization complexity and noise performance) or

* The derivation of this result is rather complex. On this basis, it is better to give the reference than to try to summarize the analysis.

non-sinusoidal phase detectors (which could decrease the acquisition time by a considerable amount and thus be desirable).

3.3 Band-Dividing Demodulation: Signal Estimation Techniques

The results of the previous sections show that the individual filter bandwidth constraints derived from signal acquisition considerations limit the performance capabilities of systems whose SNR improvement is based on the ratio of the i-f and filter bandwidths. These conclusions suggest that we direct our approach towards techniques whose SNR improvement is not strongly dependent on B_{if}/B_f at a first glance. As a simple example, consider the case where the output signal is a quantized waveform obtained by selecting the filter with the signal from the i-f bank and developing a quantum level in accordance to the filter selected. It is evident that such a technique would require a large amount of filter overlap from resolution considerations and a more promising method would consist of estimating the signal frequency from the output of more than just a single filter. The sections that follow are concerned with these interpolation techniques.

3.3.1 A Maximum Likelihood Band-Dividing FM Demodulation

This section studies the operation of an FM demodulator that uses the outputs of a bank of filters for demodulating an FM signal. After discussing the characteristics of the noise and signal terms at the outputs of these filters we describe a maximum likelihood estimator which processes the filter outputs to obtain an estimate of the desired FM.

3.3.1.1 Signal and Noise Characterization

Let $h(t)$ represent the complex envelope of the impulse response of the filter located at the "center" of the bank of filters. Then $h(t)e^{j\pi\nu t}$ represents the complex envelope of a filter removed ν cps from the center filter (assuming that our reference or "carrier" frequency for the definition of complex envelopes is chosen equal to the center frequency of the center filter). In the absence of noise the output (complex envelope) of the filter located at ν cps is given (apart from an irrelevant factor of $1/2$) by

$$Y(t, \nu) = \int S(t - \zeta) h(\zeta) e^{j\nu\zeta} d\zeta \quad (3.10)$$

where $S(t)$ is the input signal (complex envelope). Similarly the output noise is given by

$$Z(t, \nu) = \int N(t - \zeta) h(\zeta) e^{j\nu\zeta} d\zeta \quad (3.11)$$

where $N(t)$ is the input noise. If we momentarily consider the possibility of a continuum of filters, then $Y(t, \nu)$, $Z(t, \nu)$ are random processes in two independent variables (t, ν) which describe the signal and noise outputs of these filters.

Since $Z(t, \nu)$ is derived by a linear operation on $N(t)$ one may assume $Z(\cdot)$ to be a gaussian process if $N(\cdot)$ is. The autocorrelation function of $Z(t, \nu)$ is given by

$$\begin{aligned} & \overline{Z^*(t, \nu) Z(t + \tau, \nu + \Omega)} \\ &= \iint N^*(t - \zeta) N(t + \tau - \eta) h^*(\zeta) h(\eta) e^{-j2\pi [\nu\zeta - (\nu + \Omega)\eta]} d\zeta d\eta \\ &= \int R(\tau - \sigma) H(\sigma, \Omega) e^{j2\pi\nu\sigma} d\sigma \end{aligned} \quad (3.12)$$

where $R(\tau) = \overline{N^*(t) N(t + \tau)}$ is the autocorrelation function of the input noise and

$$H(\sigma, \Omega) = \int h^*(\tau - \sigma) h(\eta) e^{j2\pi\Omega\eta} d\eta \quad (3.13)$$

may be taken as the ambiguity function of the filter impulse response.

Assuming that the filter outputs are examined at the same time instant and that the noise is white with unit power density, the noise correlation function of interest is

$$\begin{aligned} \overline{Z^*(t, \nu) Z(t, \nu + \Omega)} &= H(0, \Omega) \\ &= \int |h(\zeta)|^2 e^{j2\pi\Omega\zeta} d\zeta \\ &= \int H^*(f) H(f - \Omega) df \equiv R_H(\Omega) \end{aligned} \quad (3.14)$$

where $H(f)$ is the center filter transfer function (lowpass equivalent). In view of Eq. (3.14) the process $Z(t, \nu)$ with t fixed is statistically stationary in the variable ν when the input noise is white.

We turn our attention now to the signal term $Y(t, \nu)$. We shall briefly study the conditions on the filter characteristic for an input frequency-modulated signal so that the output differs little from the quasi-stationary output. It is desirable to explicitly indicate the group delay provided by the filter (at zero frequency). Thus let

$$h(t) = k(t - \Delta) \quad (3.15)$$

where Δ is the filter phase slope at zero frequency and $k(t)$ is the impulse response of a hypothetical filter with zero phase slope at zero frequency.

In the case of FM or PM the input signal can be represented by $S(t) = e^{j\phi(t)}$ so that using this representation and Eq. (3.15) in Eq. (3.10) we find

$$\begin{aligned} Y(t, \nu) &= \int e^{j[\phi(t - \zeta) + 2\pi\nu\zeta]} k(\zeta - \Delta) d\zeta \\ &= e^{j[\phi(t - \Delta) + 2\pi\nu\Delta]} \int e^{j[\phi(t - \zeta - \Delta) - \phi(t - \Delta)] + j2\pi\nu\zeta} k(\zeta) d\zeta \end{aligned} \quad (3.16)$$

and upon using the definition

$$R(t, \zeta) = \phi(t - \zeta) - \phi(t) + \zeta \dot{\phi}(t) \quad (3.17)$$

we find that

$$Y(t, \nu) = e^{j[\phi(t - \Delta) + 2\pi\nu\Delta]} K\left(\nu - \frac{\dot{\phi}(t - \Delta)}{2\pi}\right) + E(t, \nu) \quad (3.18)$$

where

$K(\cdot)$ is the transform of $k(t)$ and

$$E(t, \nu) = e^{j[\phi(t - \Delta) + 2\pi\nu\Delta]} \int e^{j\zeta[2\pi\nu - \dot{\phi}(t - \Delta)]} \left[e^{jR(t - \Delta, \zeta)} - 1 \right] R(\zeta) d\zeta. \quad (3.19)$$

It may be recognized that the first term in Eq. (3.18) is the quasi-stationary portion of the output signal. The magnitude of the error term is bounded as follows

$$\begin{aligned}
 |E(t, \nu)| &\leq \int \left| e^{jR(t-\Delta, \zeta)} - 1 \right| |k(\zeta)| d\zeta \\
 &= \int 2 \left| \sin \frac{R(t-\Delta, \zeta)}{2} \right| |k(\zeta)| d\zeta.
 \end{aligned} \tag{3.20}$$

so that a sufficient condition for small distortion assuming $K(0) = 1$ is

$$\left| R(t-\Delta, \zeta) \right| \ll 1 \text{ for } -\frac{T}{2} < \zeta < \frac{T}{2} \tag{3.21}$$

where $|k(t)|$ is assumed to be negligible for t outside an interval of duration T centered on $t = 0$. Assuming that the indicated derivatives exist, then $R(t, \zeta)$ has the expansion

$$R(t, \zeta) = \sum_{n=2}^N \frac{(-\zeta)^n}{n!} \frac{d^n \phi(t)}{dt^n} + \frac{(-\zeta)^N}{N!} \frac{d^N \phi(\theta)}{d\theta^N}; \quad t - \zeta < \theta < t \tag{3.22}$$

which leads to the sufficient condition

$$\frac{\zeta^2}{2} \left| \frac{d^2 \phi(\theta)}{d\theta^2} \right| \ll 1 \text{ for } -\frac{T}{2} < \zeta < \frac{T}{2}, \quad t - \zeta < \theta < t. \tag{3.23}$$

and least tight condition is clearly*

$$\text{Max} \left| \frac{d^2 \phi(t)}{dt^2} \right| \ll \frac{2}{T^2} \tag{3.24}$$

For the case of sinusoidal modulation given by $\phi(t) = \delta \sin \omega_m t$ then Eq. (3.24) becomes after a slight rearrangement

$$f_m^2 T^2 \ll \frac{1}{2\delta\pi^2} \tag{3.25}$$

so that for a large modulation index the product $f_m T$ must be very much less

* When $\phi(t)$ is a random process Eq. (3.23) and Eq. (3.24) are not so convenient. In such a case one should replace Eq. (3.21) by

$$\sqrt{|R(t-\Delta, \zeta)|^2} \ll 1, \quad -\frac{T}{2} < \zeta < \frac{T}{2}.$$

than one if the sufficient quasi-stationary condition Eq. (3.24) is to hold for sinusoidal modulation. Even for values of δ of the order of unity Eq. (3.24) implies that $f_m T \ll 1$.

3.3.1.2 Signal Estimation

In terms of the hypothetical filter with zero group delay we may represent the output of a filter with center frequency γ as

$$w(t, \nu) = \left[Z(t, \nu) + e^{j\phi(t-\Delta)} K\left(\nu - \frac{\phi(t-\Delta)}{2\pi}\right) \right] \exp[j2\pi\nu\Delta] \quad (3.26)$$

where the noise

$$Z(t, \nu) = \int N(t - \zeta - \Delta) k(\zeta) e^{j2\pi\nu\zeta} d\zeta \quad (3.27)$$

has correlation function

$$\overline{Z^*(t, \nu) Z(t, \nu + \Omega)} = \int K(f) K^*(f + \Omega) df \quad (3.28)$$

assuming $N(t)$ to be white and of unit spectral density.

If $2N + 1$ equally spaced filters are available we may state our estimation problem as follows: given the $2N + 1$ random processes $w(t, kF)$; $k = 0, \pm 1, \dots, \pm N$, then determine the frequency modulation $\dot{\phi}(t)/2\pi$.

An obvious heuristic solution to this problem arises from the observation that the magnitude of the signal component in Eq. (3.26) has a maximum at

$$\nu(t) = \nu_{\max} + \frac{\dot{\phi}(t-\Delta)}{2\pi} \quad (3.29)$$

where

$$\max_{\nu} |K(\nu)| = |K(\nu_{\max})|. \quad (3.30)$$

Assuming a symmetrical unimodal filter

$$\nu_{\max} = 0 \quad (3.31)$$

and the signal component has its maximum magnitude at the filter whose center frequency equals the "instantaneous" frequency of the input. Thus, neglecting

noise, one possible estimation procedure is to determine $|w(t, kF)|$ and by an interpolation procedure estimate the value of ν for which $|w(t, \nu)|$ is maximum. This value of ν , say $\tilde{\nu}(t)$, will be an estimate of $\dot{\phi}(t - \Delta) / 2\pi$.

Unfortunately there is no proof that this procedure will result in an optimum estimate of the input frequency modulation. We shall determine an optimum procedure for the particular case in which the outputs of the $2N + 1$ filter are examined at the same time instant, i. e., a no-memory processing of the filter outputs. For convenience in notation let

$$\begin{aligned} Z(t, \nu) &= Z(\nu) \\ \phi(t - \Delta) &= \phi \\ \frac{\dot{\phi}(t - \Delta)}{2\pi} &= \zeta \\ w(t, \nu) &= w(\nu) \end{aligned} \quad (3.32)$$

so that

$$W(\nu) = w(\nu) e^{-j2\pi\nu\Delta} = z(\nu) + e^{j\phi} K(\nu - \zeta) \quad (3.33)$$

Since Δ is known we may assume that $w(\nu) e^{-j2\pi\nu\Delta} \equiv W(\nu)$ is observed rather than $w(\nu)$ alone. A study of Eq. (3.33) reveals that if $w(\nu) e^{-j2\pi\nu\Delta}$ were known for all values of ν , the problem of estimating ζ would be formally identical to the problem of determining the position of a pulse of known shape but unknown phase (assuming ϕ unknown) and position in stationary colored gaussian noise of autocorrelation function given by Eq. (3.28).

Since $w(\nu)$ is known only for a finite set of values of ν our problem is a sampled version of the above problem, namely: determine the position of a pulse of unknown phase and position in stationary colored gaussian noise by observation of a finite number of periodically spaced samples.

Using vector and matrix notation, we define the observed filter outputs and the signal and noise terms as

$$\bar{W} = \begin{bmatrix} \cdot \\ \cdot \\ \cdot \\ W(F) \\ W(o) \\ W(-F) \\ \cdot \\ \cdot \\ \cdot \end{bmatrix} \quad (3.34)$$

$$\bar{Z} = \begin{bmatrix} \cdot \\ \cdot \\ \cdot \\ Z(F) \\ Z(o) \\ Z(-F) \\ \cdot \\ \cdot \\ \cdot \end{bmatrix} \quad (3.35)$$

$$\bar{K}(\zeta_o) = \begin{bmatrix} \cdot \\ \cdot \\ \cdot \\ K(F-\zeta_o) \\ K(-\zeta_o) \\ K(-F-\zeta_o) \\ \cdot \\ \cdot \\ \cdot \end{bmatrix} \quad (3.36)$$

so that the observed vector \bar{W} is given by

$$\bar{W} = \bar{Z} + e^{j\phi} \overline{K(\zeta_0)} \quad (3.37)$$

when the parameter value $\zeta = \zeta_0$.

This problem of optimally estimating ζ may be solved in two steps. First one may determine a linear transformation of the set of samples (i. e., \bar{W}) which will yield independent noises and then one may solve the simpler independent noise case. Since the linear transformation is reversible no information is lost and the overall optimization problem will remain unchanged if we deal with the transformed variables. Let the noise whitening transformation be denoted by T , the transformed samples by \bar{W}' , and the transformed noises by \bar{Z}' . Then

$$\bar{W}' = \bar{Z}' + e^{j\phi} T \overline{K(\zeta_0)} \quad (3.38)$$

where

$$\begin{aligned} \bar{W}' &= T \bar{W} \\ \bar{Z}' &= T \bar{Z}, \end{aligned} \quad (3.39)$$

In the transformed problem the noises are independent and the optimization problem is considerably simplified. Standard statistical techniques may be used to obtain minimum mean squared error or maximum likelihood estimates. Thus it may be shown that the maximum likelihood estimate of ζ is given by $\tilde{\zeta}$ below,

$$\tilde{\zeta} = \text{Max}_{\zeta} \left\{ \ln I_0 \left[\left| \sum_{-N}^N w'_k s_k^*(\zeta) \right| \right] - \sum_{-N}^N |s_k(\zeta)|^2 \right\} \quad (3.40)$$

where $\{s_k(\zeta)\}$ are the elements of $T \overline{K(\zeta)}$

$$TK(\zeta) = \begin{bmatrix} \cdot \\ \cdot \\ \cdot \\ s_1(\zeta) \\ s_0(\zeta) \\ s_{-1}(\zeta) \\ \cdot \\ \cdot \\ \cdot \end{bmatrix} \quad (3.41)$$

and $\{w_k\}$ are the elements of $\overline{W'}$,

$$\overline{W'} = \begin{bmatrix} \cdot \\ \cdot \\ \cdot \\ w_1' \\ w_0' \\ w_{-1}' \\ \cdot \\ \cdot \\ \cdot \end{bmatrix} \quad (3.42)$$

The first sum in Eq. (3.40) represents a determination of the correlation between the transformed input and expected signal while the second term is a bias term depending upon the energy of the transformed signal vector. The function $I_0[\cdot]$ is the modified Bessel function of the first kind and order zero. One may interpret the operations $\ln I_0(\cdot)$ as a nonlinear envelope detection operation.

A block diagram of the maximum likelihood estimator is shown in Fig. 5. Since this estimator processes the filter bank outputs at the same time instant, i.e., since it is a no-memory processing, further processing which involves filtering operations can be expected to reduce the noise still further. The most obvious processing of $\tilde{\zeta}(t)$ would be a straightforward filtering to the known bandwidth of $\dot{\phi}(t)$.

One may formulate a more involved optimal estimation problem that involves general processing of the filter bank outputs with memory. It appears that such processing is too complicated to be of practical importance. Even the scheme of Fig. 5 is rather involved. There is one special situation in which the operations in Fig. 5 simplify, namely, when the impulse responses (and thus transfer functions) of the filters are orthogonal. In such a case the noises at the filters outputs become independent and the transformation T is unnecessary.

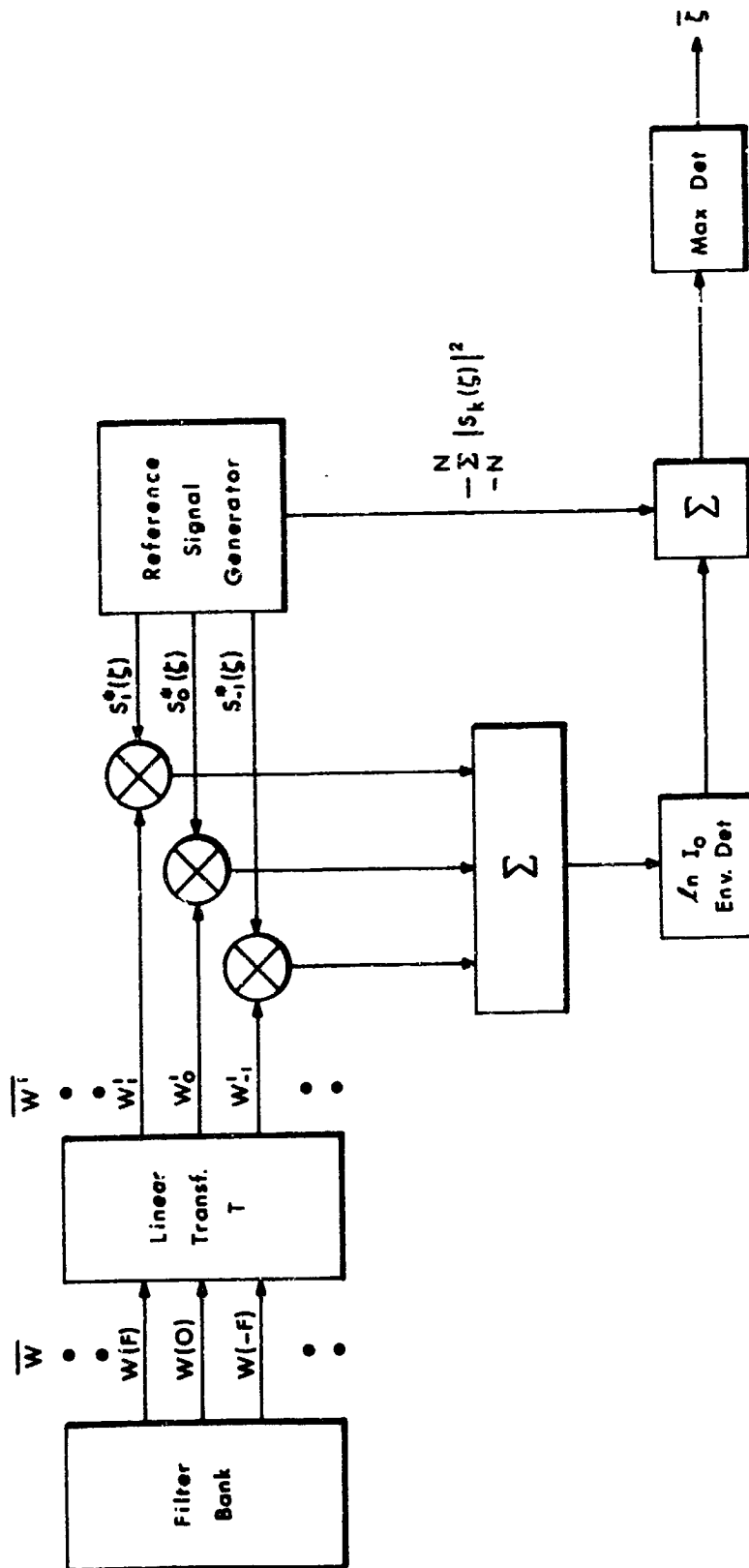


Fig.5 Block diagram of maximum likelihood estimator (case of no-memory processing).

If in addition N is chosen large enough so that the set of values $\{K(k-\zeta); k = 0, \pm 1, \dots, \pm N\}$ represents a closely sampled version of $K(\nu-\zeta)$ for any expected range of values of ζ then the bias term becomes independent of ζ and may be removed. Also since $\ln I_0[x]$ is monotonically related to x a simple envelope detector will be satisfactory.

3.3.2 A Simple Interpolation Scheme

If the above procedures are too complicated it might be advisable to consider a simple interpolation scheme which examines the set $\{|w(t, kF)|; k = 0, \pm 1, \dots, \pm N\}$ of envelope detected outputs from the filter bank and forms a smooth curve approximating $|w(t, \nu)|$. The value of ν at which this approximant has its maximum would then be an estimate of $\dot{\phi}(t-\Delta)/2\pi$. For such a procedure to be effective the frequency separation F between adjacent filter center frequencies should be sufficiently small so that $K(\nu)$ varies little for changes in ν of this order of magnitude. In addition, of course, the SNR must be sufficiently high.

We consider a quadratic interpolation scheme which involves passing a third degree polynomial through three adjacent points. There is no need to do this for all triplets of points but only for the triplet which surrounds the desired maximum. Thus one may first determine the filter whose envelope is maximum and then select as the desired triplet the outputs of this filter and the adjacent filters. In the event that the maximum envelope output occurs at one of the two end filters, the two adjacent interior filters should be used. Our discussion ignores this end point situation which is readily handled by slight modifications of the procedure discussed below.

Since the interpolation operation is a no-memory operation, we need not introduce time in our discussion and we may use the abbreviated notation of Eqs. (3.32) - (3.34). Let

$$E(\nu) \equiv |W(\nu)| \quad (3.43)$$

be the continuous function which is sampled by the filter output envelopes. For convenience in discussion, suppose that the desired triplet of filters is centered on $\nu = 0$ and let

$$\begin{aligned} E(-F) &\equiv E_- \\ E(0) &\equiv E_0 \\ E(F) &\equiv E_+ \end{aligned} \quad (3.44)$$

Then, if $f(\nu) = a\nu^2 + b\nu + c$ is the quadratic passing through the points $(E_-, -F)$, $(E_0, 0)$ and (E_+, F) , it satisfies the equations

$$\begin{aligned} E_- &= aF^2 - bF + c \\ E_0 &= c \\ E_+ &= aF^2 + bF + c \end{aligned} \quad (3.45)$$

The coefficient c is given directly and the coefficients a and b are readily computed as

$$\begin{aligned} b &= \frac{E_+ - E_-}{2F} \approx \left[\frac{dE(\nu)}{d\nu} \right]_{\nu=0} \equiv \dot{E}(0) \\ a &= \frac{(E_+ - E_0) - (E_0 - E_-)}{2F^2} \approx \frac{1}{2} \left[\frac{d^2E(\nu)}{d\nu^2} \right]_{\nu=0} \equiv \frac{1}{2} \ddot{E}(0) \end{aligned} \quad (3.46)$$

where the approximations indicated are valid for sufficiently small F .

One may readily determine that the maximum value of $f(\nu)$ occurs at

$$\nu = -\frac{b}{2a} = \frac{F}{2} \left[\frac{E_- - E_+}{E_+ + E_- - 2E_0} \right] \approx -\frac{\dot{E}(0)}{\ddot{E}(0)} \quad (3.47)$$

It follows from the above that if the filter which has the maximum output envelope has a center frequency located at $\nu = kF$, the location of the maximum of the interpolated function, $\hat{\nu}$, is given by

$$\hat{\nu} = F \left[K + \frac{1}{2} \cdot \frac{E_- - E_+}{E_+ + E_- - 2E_0} \right] \quad (3.48)$$

3.3.3 Effect of Mis-Selection Noise in Systems with Filter Overlap

In any band-dividing technique which selects the filter with maximum output, and regardless of whether or not a more refined estimate is subsequently made, noise power is produced due to filter mis-selection. Akima calculates this mis-selection noise power for a system in which the band-dividing channels are orthogonal. He assumes that the correct channel is selected with probability q and each of the remaining $N-1$ channels have probability p of being mistakenly selected. The result of his calculation is that the mis-selection noise power is given by

$$P_{n2} = \frac{N_p (N^2 - 1)}{12} \quad (3.49)$$

As a first attempt, we will modify the problem by assuming that the two channels adjacent to the correct channel have higher probability of being mis-selected than more remote channels. This is a good representation of the situation where the frequency responses of adjacent filters are overlapping to some extent. Thus, we let

- q_c = probability of selecting the correct channel
- q_a = probability of selecting either adjacent channel
- p' = probability of selecting either one of the other channels.

With these assumptions we will calculate a new value of noise power P_{n2}' and compare this with Akima's result. First we will compute the expected value of the channel number actually chosen (\bar{i}), assuming that the signal actually occurs in the j^{th} channel.

$$\begin{aligned} \bar{i} = [1 + 2 + \dots + N - (j - 1) - j - (j + 1)] p' \\ + (j - 1) q_a + j q_c + (j + 1) q_a \end{aligned} \quad (3.50)$$

or,

$$\bar{i} = \frac{N(N+1)}{2} p' - 3 j p' + j (q_c + 2 q_a) \quad (3.51)$$

Now we use the fact that

$$(N - 3) p' + q_c + 2q_a = 1 \quad (3.52)$$

to eliminate the quantity $q_c + 2q_a$ with the result

$$\bar{i} - \frac{N+1}{2} = (j - \frac{N+1}{2}) (1 - Np') \quad (3.53)$$

This is the same result as Akima's, except that we have replaced p with p' , and some consideration can show that this could have been predicted from the symmetry of our probability assignment.

Next we note that, as in Akima's work,

$$P'_{n2} = \overline{(i - \bar{i})^2} = \overline{i^2} - \bar{i}^2 \quad (3.54)$$

$$= \left[1^2 + 2^2 + \dots + N^2 - (j-1)^2 - j^2 - (j+1)^2 \right] p' + (j-1)^2 q_a + j^2 q_c + (j+1)^2 q_a - \bar{i}^2 \quad (3.55)$$

Expanding and collecting, with the use of Eq. (3.52) and the relationship

$$1^2 + 2^2 + \dots + N^2 = \frac{N}{6} (N+1) (2N+1), \quad (3.56)$$

we have

$$P'_{n2} = \frac{N}{6} (N+1) (2N+1) p' + j^2 (1 - Np') + \bar{i}^2 + 2(q_a - p). \quad (3.57)$$

Now we restrict ourselves, as Akima did, to the noise power in the absence of modulation. Hence,

$$j = \frac{N+1}{2}. \quad (3.58)$$

This in turn implies, from Eq. (3.53) that

$$\bar{i} = \frac{N+1}{2}. \quad (3.59)$$

Substituting these two relations in Eq. (3.57) we find

$$P'_{n2} = \frac{Np'(N^2-1)}{12} + 2(q_a - p'). \quad (3.60)$$

This is the desired result and for purposes of comparison we form the ratio of P'_{n2} and P_{n2} (from Eq.(3.49)):

$$\frac{P'_{n2}}{P_{n2}} = \frac{p'}{p} \left[1 - \frac{24}{N(N^2-1)} \right] + \frac{24}{N(N^2-1)} \frac{q_a}{p}. \quad (3.61)$$

When this ratio is greater than one, performance of the system with overlap is inferior to performance of the system without, when the ratio is less than one the reverse is true. We note that with Eq. (3.61) and Eq. (3.52) we have four variables, p'/p , q_a/p , q_c/p , and P'_{n2}/P_{n2} , any two of which may be considered independent. In Fig. 6 we treat p'/p and q_a/p as the independent variables and only the contour $P'_{n2}/P_{n2} = 1$ is drawn so that curves for various values of N may be included. Above this contour (for a given N) performance of the system with overlap is inferior to the system without; below the contour it is superior.

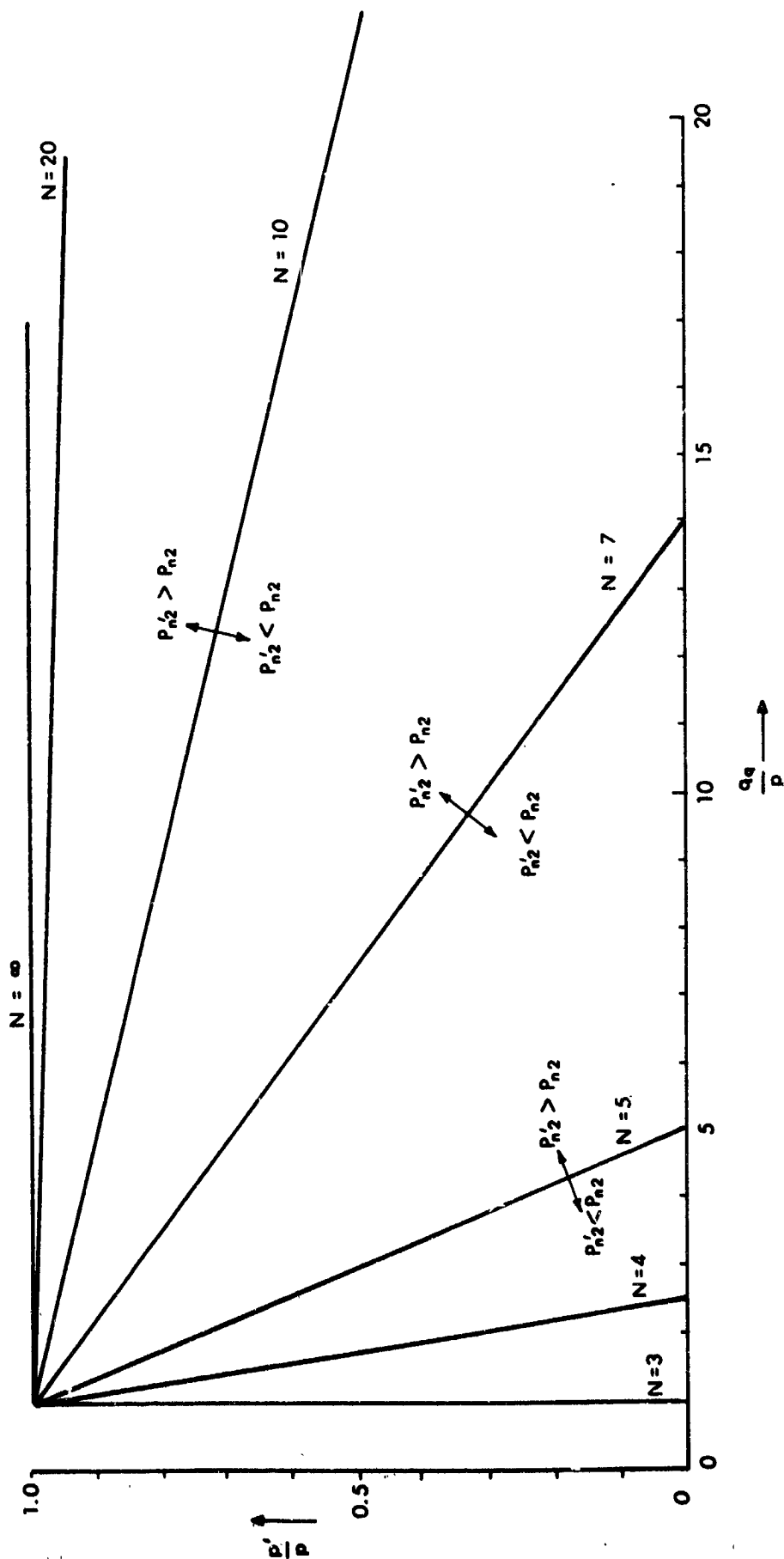


Fig. 6 Contours of $\frac{P'_{n2}}{P_{n2}} = 1$, for various N .

REFERENCES FOR SECTION III

1. Akima, H., "Theoretical Studies on S/N Characteristics of an FM System", IEEE Trans. on SET, December 1963.
2. ADCOM, Inc., "Advanced Threshold Reduction Techniques Study" First Quarterly Progress Report, Contract No. NAS 5-9011, September 1964.
3. Richman, D., "Color-Carrier Preference Phase Synchronization in NTSC Color TV", Proc. IRE, January 1954.
4. Viterbi, A. J., "Acquisition and Tracking Behavior of PLL's", J. P. L., Ext. public. 673, July 1959.
5. ADCOM, Inc., "High Accuracy Satellite Tracking Systems", Ninth Quarterly Progress Report, Contract No. NAS 5-1187, June 1963.

IV. EXPERIMENTAL RESULTS

The present section discusses the experimental effort up to date and includes some sample curves of conventional and second order PLL demodulator performance, as well as a discussion of the results.

4.1 The Automatic Threshold Curve Plotter

The automatic test system is essentially similar to that presented in the First Quarterly Progress Report. The system provides a direct comparison of the threshold characteristics of a test demodulator to those of a conventional one to better than ± 0.5 db. Its performance has been successfully checked.

A block diagram of the test system is shown in Fig. 7. The sinusoidal FM signal is generated from an ultrastable audio oscillator, added to wideband noise and filtered with a four-pole filter whose bandwidth may be selected to fit the signal characteristics as desired. This composite i-f signal feeds a linear driver amplifier having a peak capability of + 20 db, and is then demodulated.

The composite baseband output is filtered by a LPF whose bandwidth is also adjustable to the signal characteristics. The signal level is held constant with an AGC loop within ± 0.1 db. The resultant output is notch-filtered to separate the signal and its harmonics from the noise and the resultant spectrum is detected on an audio logarithmic amplifier so that its output is proportional to audio SNR and directly readable in db. This output forms the Y-axis of the X-Y plotter.

Meanwhile, the noise level of the composite input is controlled by feeding the wideband noise into a linear-to-db, continuously-adjusted attenuator which is swept at 0.2 db per sec by a motor, and a d-c signal proportional to the db attenuation provides direct calibration of the input SNR and forms the Y-axis of the X-Y plotter.

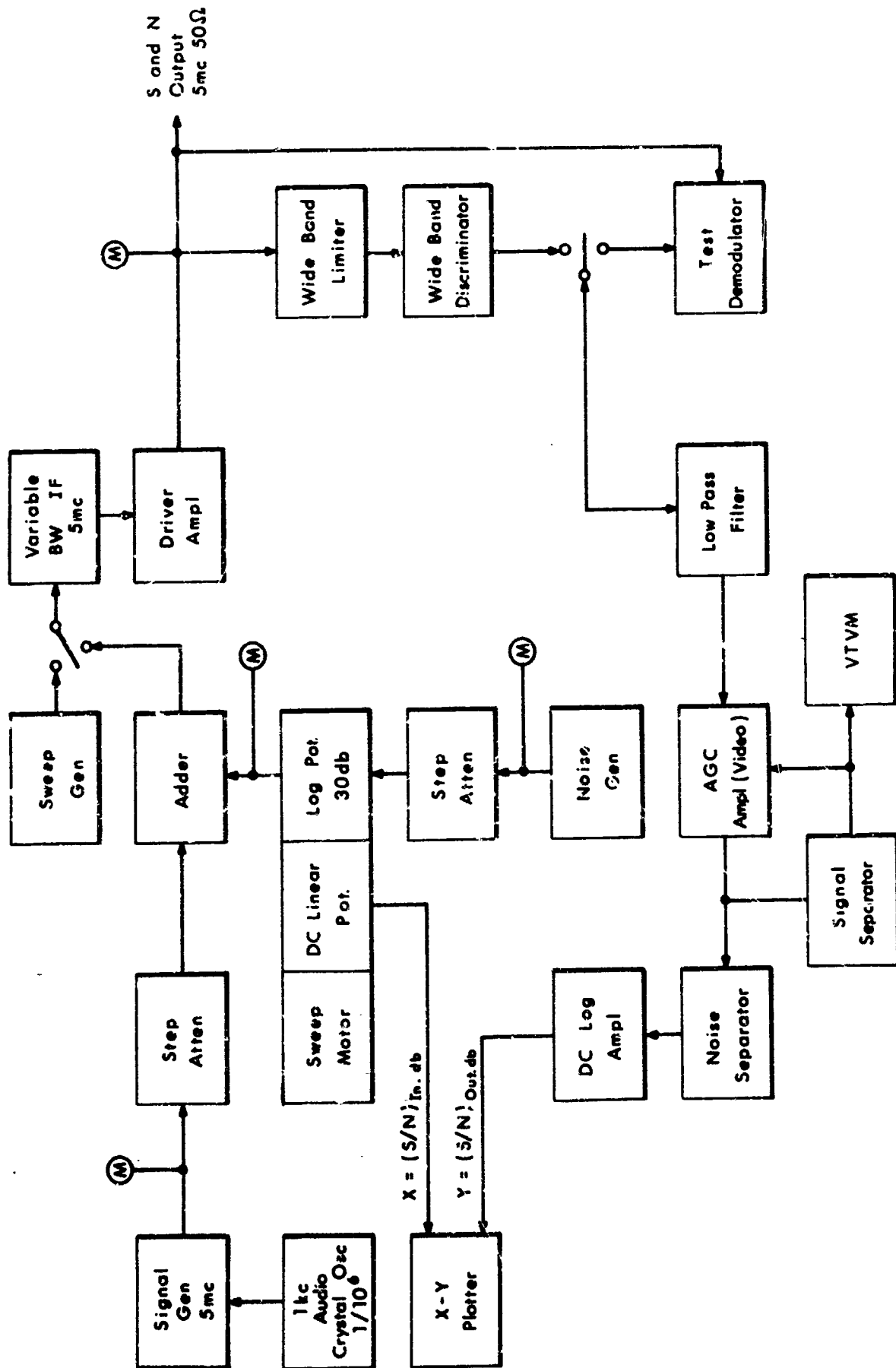


Fig 7 Block diagram of automatic test system.

Monitoring is done throughout the system to assure that the periodic calibrations hold constant for the duration of the test of interest.

The choice of i-f bandwidths for given modulation characteristics is now discussed. For a sinusoidal modulation of index δ and frequency ω_m rad/sec, the required i-f bandwidth is selected in accordance to a preset distortion criterion. The common rule of thumb of $2(\delta + 1)f_m$ cps approximates a 10% distortion requirement and becomes improper for tighter tolerances. If the distortion required is between 1-10%, the aforesaid rule will require a correction factor smaller than 2 for indices $\delta > 1$. The test system uses i-f filters with 3 db bandwidths of 20, 50, 100 and 200 kc which should be sufficient to span the range of $\delta = 1 - 100$ for $f_m = 1$ kc.

4.2 The Second Order PLL

A block diagram of the second order loop is shown in Fig. 8 and the circuit diagram in Fig. 9. The transformer turns ratio in the phase detector is chosen for maximum sensitivity while still maintaining the number of secondary turns below self-resonance, the sensitivity in question being 1.5 volts per rad. Meanwhile, the VCO uses a variable capacitance diode in a parallel tuned oscillator circuit, this diode in question chosen for its linear characteristic and reverse biased to the center of its linear region. A field effect transistor is also used in the VCO to provide a high input impedance to the tuned circuit. The amplification stages that follow provide isolation and gain to produce 1 v rms into the 50Ω phase detector input impedance. The overall VCO linearity is shown in Fig. 10 while its amplitude vs frequency characteristics is shown in Fig. 11. The VCO sensitivity is 500 kc/volt.

The loop filter design is now presented. The lag network transfer function can be written in terms of the (K, B_n, a) parameters introduced in the First Quarterly Progress Report as

$$F(s) = \frac{1 + \tau_1 s}{1 + \tau_2 s} = \frac{1 + \frac{s}{a B_n}}{1 + \frac{s K}{a(2-a)B_n^2}}, \quad \frac{K}{B_n} \gg a \quad (4.1)$$

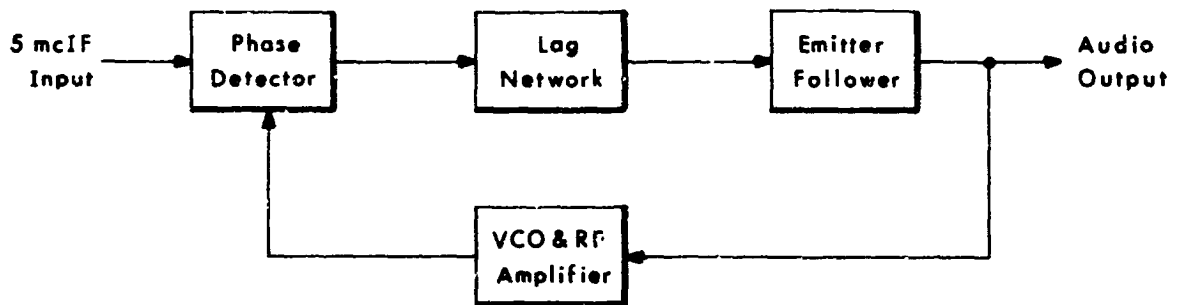


Fig. 8 Block diagram of second order PLL.

where $\tau_1 = R_2 C$ and $\tau_2 = (R_1 + R_2) C$. It was shown in this report that optimum performance for a sinusoidal modulation of index δ and frequency ω_m rad/sec is achieved by using

$$a = 1 \quad (4.2)$$

$$B_n = \left(\frac{5\delta}{\phi_c} \right)^{1/2} \omega_m \text{ cps} \quad (4.3)$$

where ϕ_c is the critical phase error in rad and the following approximations are assumed:

$$\frac{K}{B_n} \gg 2a \quad (4.4)$$

$$\left(\frac{K}{B_n} \right)^2 \gg a^2 (2-a)^2 \left(\frac{B_n}{\omega_m} \right)^2 \quad (4.5)$$

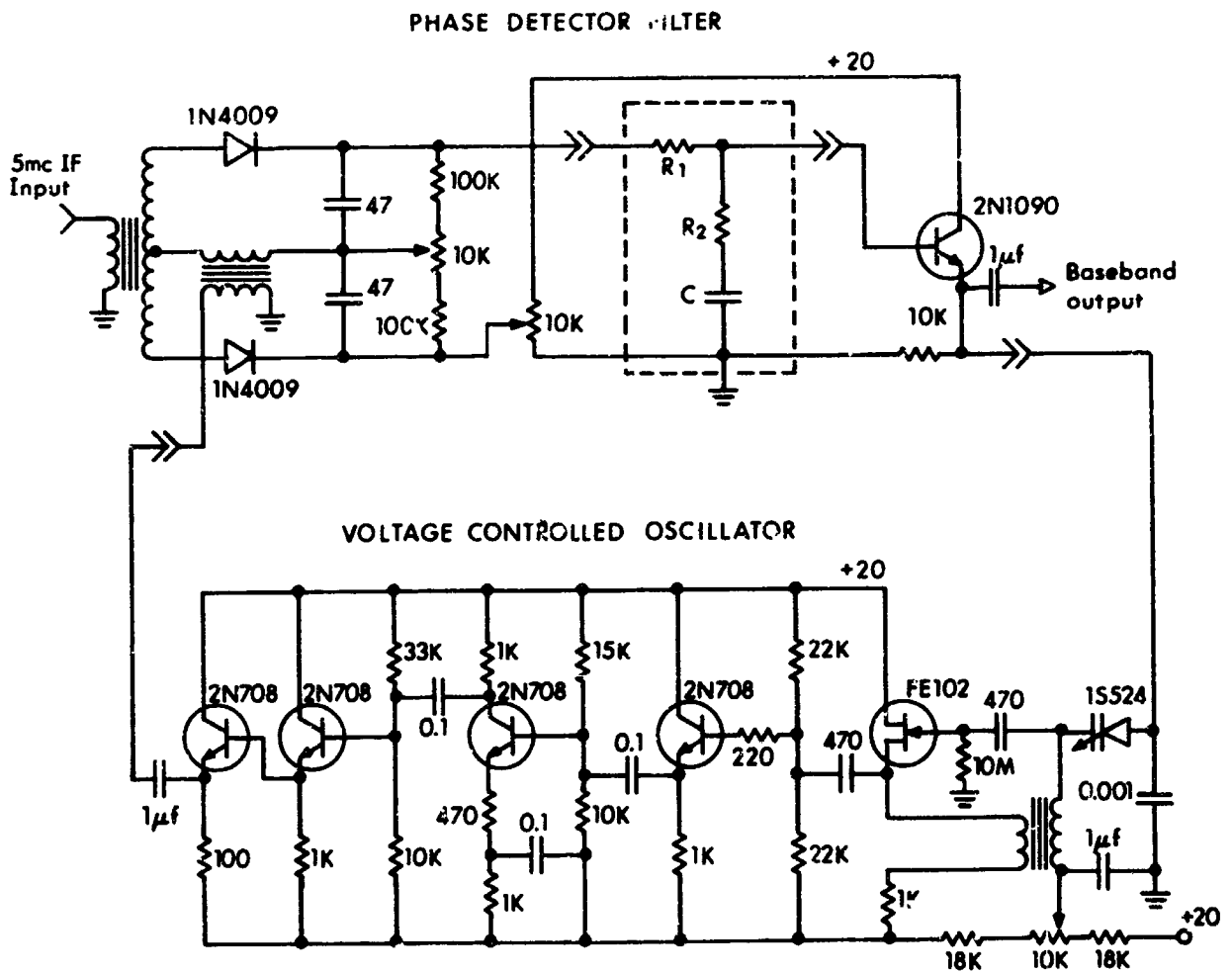


Fig. 9 Schematic of PLL.

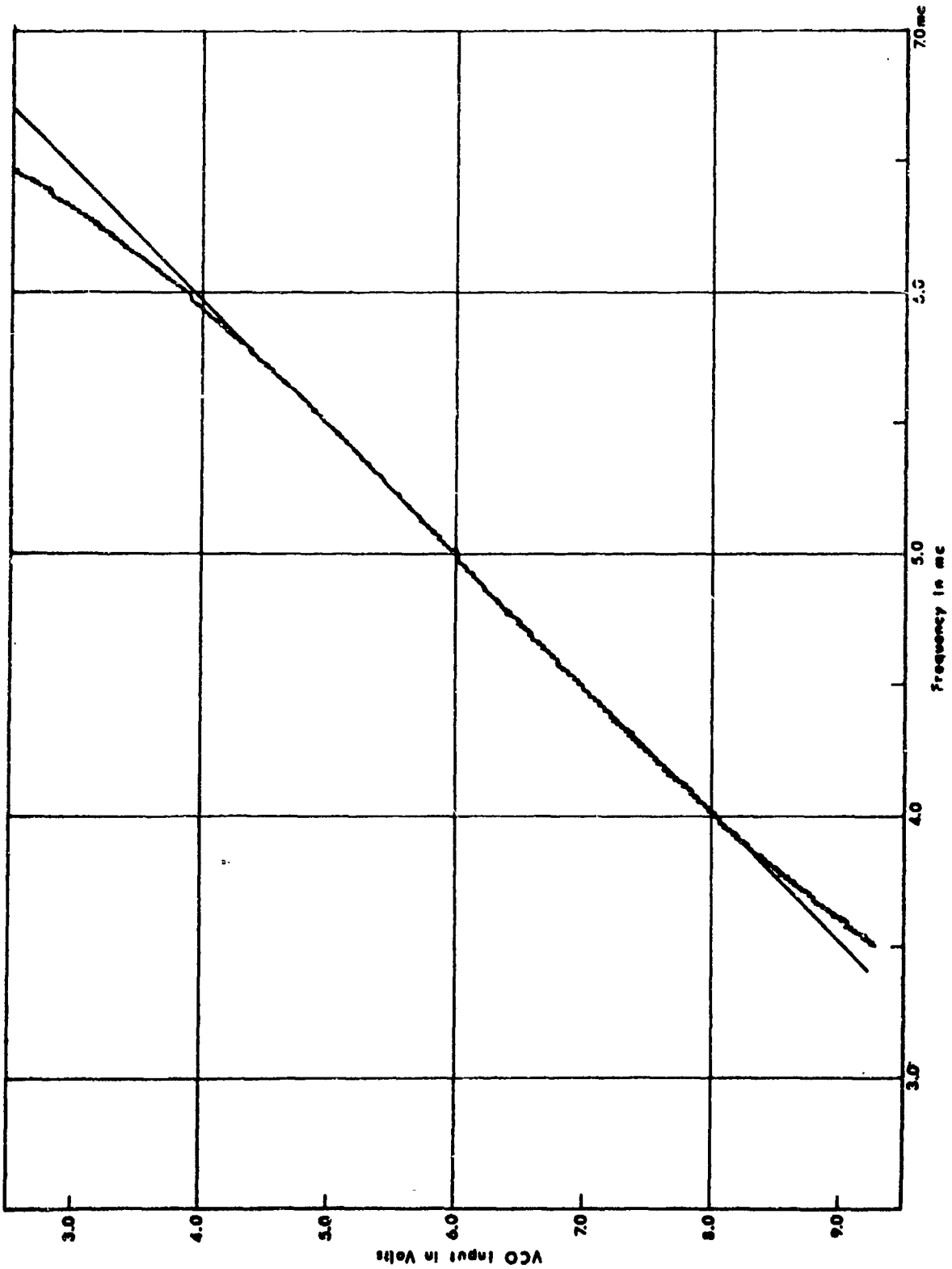


Fig. 10 VCO linearity.

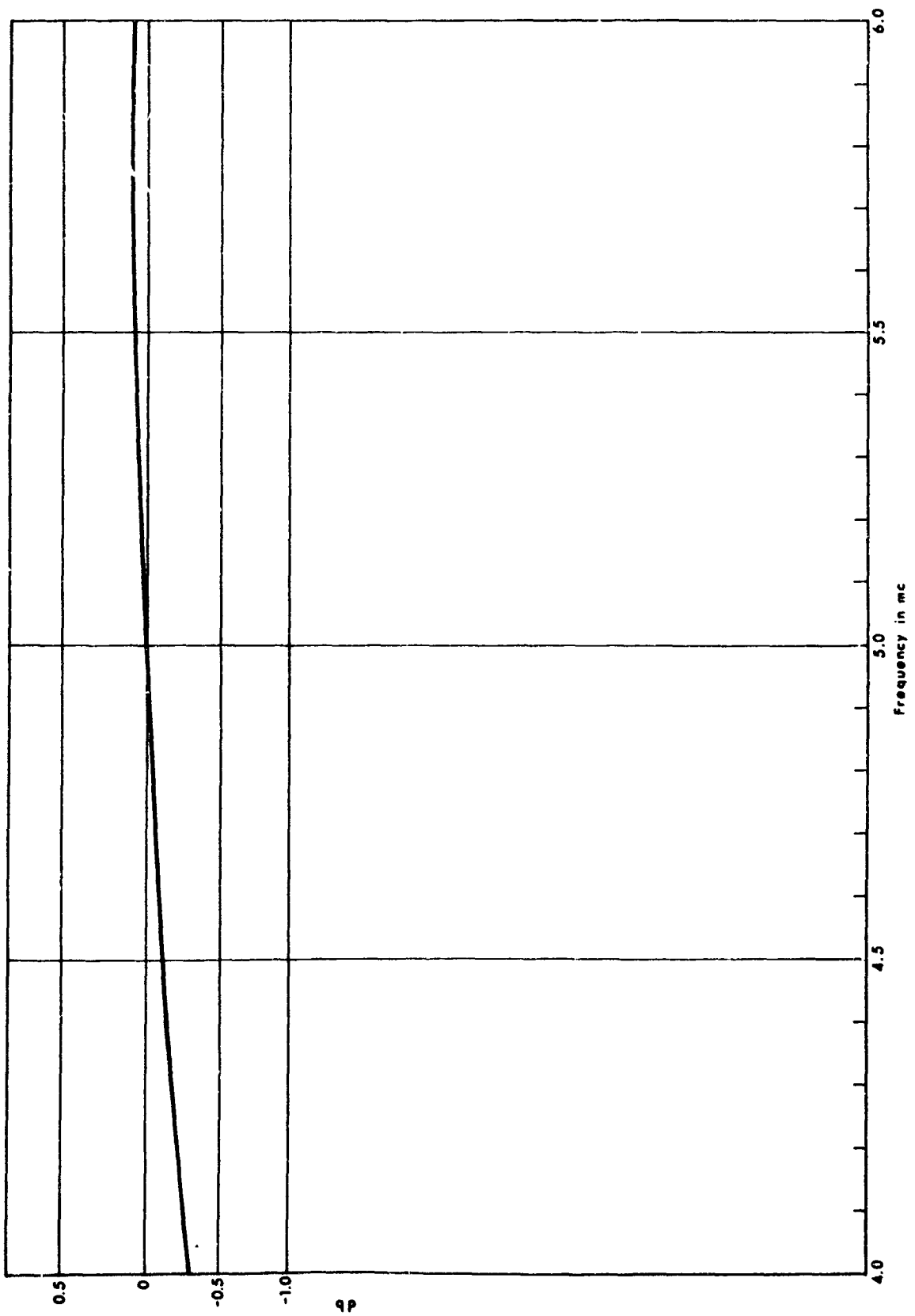


Fig. 11 VCO amplitude vs. frequency.

$$\left(\frac{B_n}{\omega_m}\right)^4 \gg \frac{1}{|2-3a|} \left(\frac{B_n}{\omega_m}\right)^2 \gg \frac{1}{a^2(2-a)} \quad (4.6)$$

For the case where $\omega_m = 2\pi \times 10^3$ rad/sec $a\phi_c = \pi/2$, and $\delta = 10, 20, 30$, the loop filter design governed by Eqs. (4.1) - (4.6) can be summarized as follows:

δ	B_n	$K >$	τ_1	τ_2
10	35.6 kc	7.1×10^5	2.81×10^{-5}	$K\tau_1^2$
20	50.2 kc	12.1×10^5	1.99×10^{-5}	$K\tau_1^2$
30	60.8 kc	17.7×10^5	1.64×10^{-5}	$K\tau_1^2$

The experimental threshold curves for these systems are shown in Figs. 12 - 14 where the second order PLL performance (PLL_2) is compared to that of a conventional demodulator (STD) for the specified test conditions. The threshold reduction capabilities of the second order PLL are evident for $\delta = 30$, and they disappear as the index gets smaller. This behavior is compatible with the analytical results. The second order PLL threshold was characterized in the First Quarterly Progress Report as

$$\frac{S}{\Phi} \geq \frac{1.75F^2}{\phi_c^{5/2}} \delta^{1/2} \omega_m \quad (4.7)$$

where F is the noise error crest factor and ϕ_c the critical peak phase error that characterizes the threshold in accordance to the noise error statistics. An analogous expression for a conventional FM demodulator reads

$$\frac{S}{\Phi} \geq \gamma B_{if} \quad (4.8)$$

where γ is the input SNR at threshold and B_{if} is the input noise bandwidth in cps.

The i-f bandwidth required to pass a given sinusoidal modulation depends on the distortion tolerance as discussed in the previous section. The actual

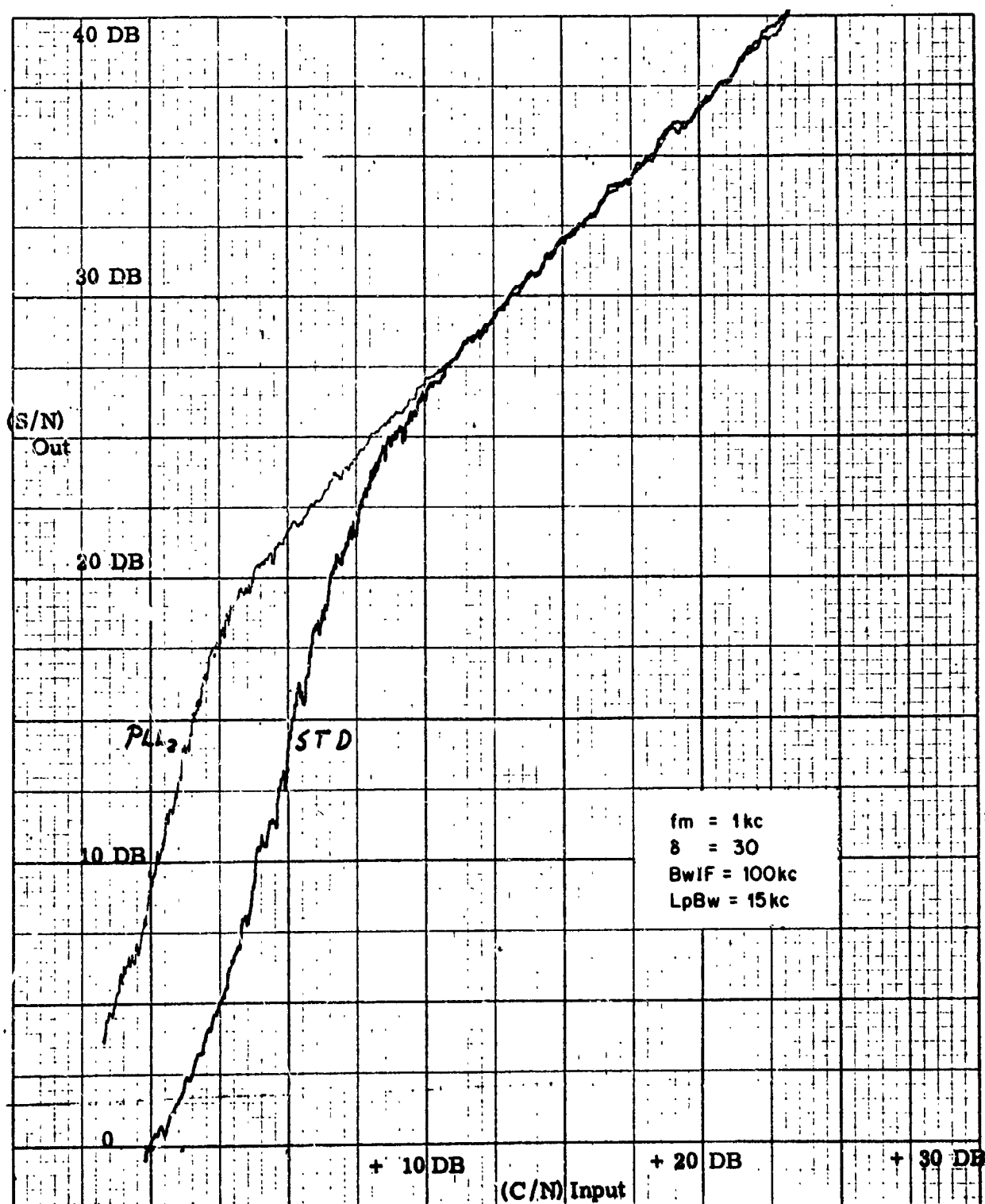


Fig. 12 Second order PLL performance for $\delta = 30$.

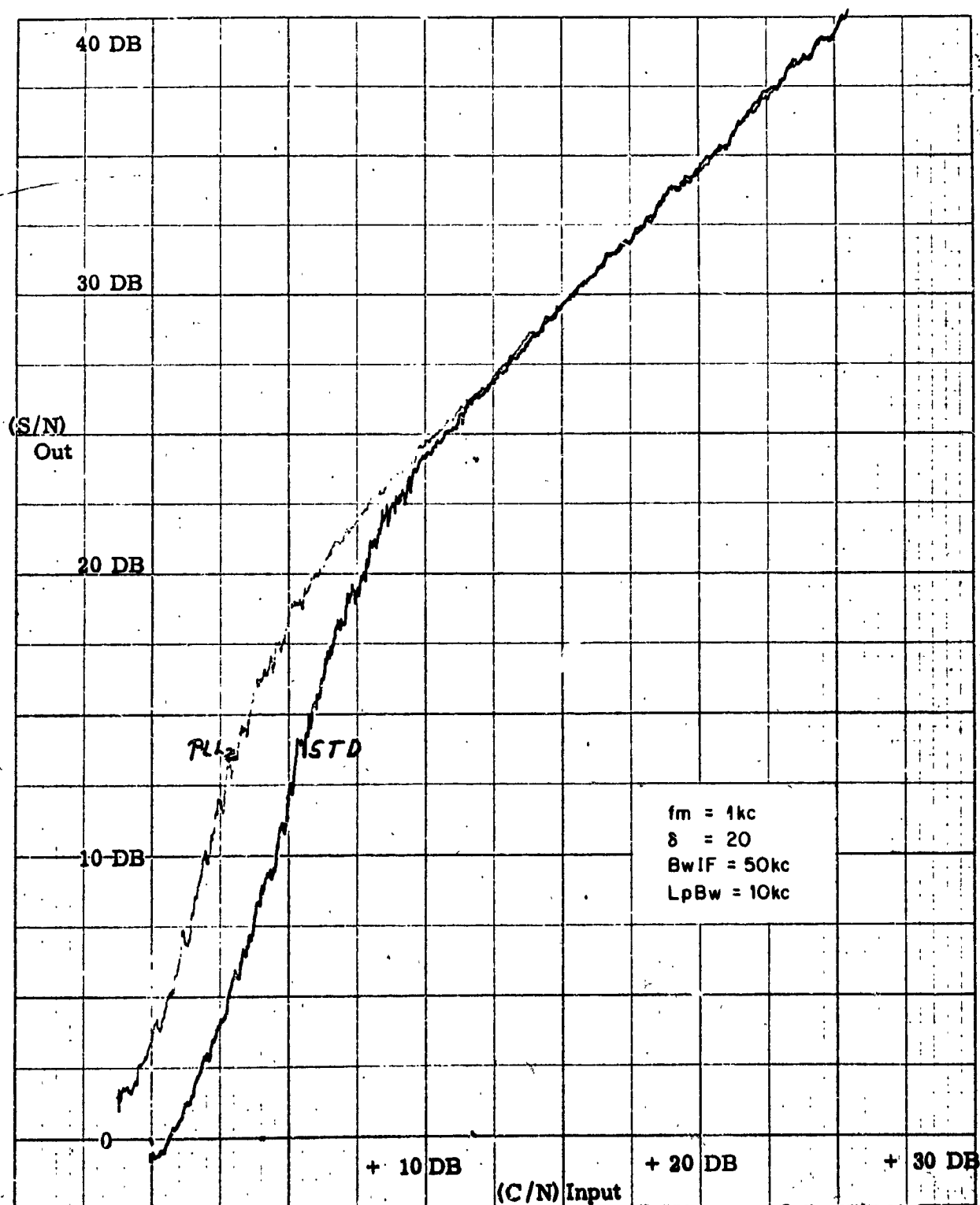


Fig. 13 Second order PLL performance for $\delta = 20$.

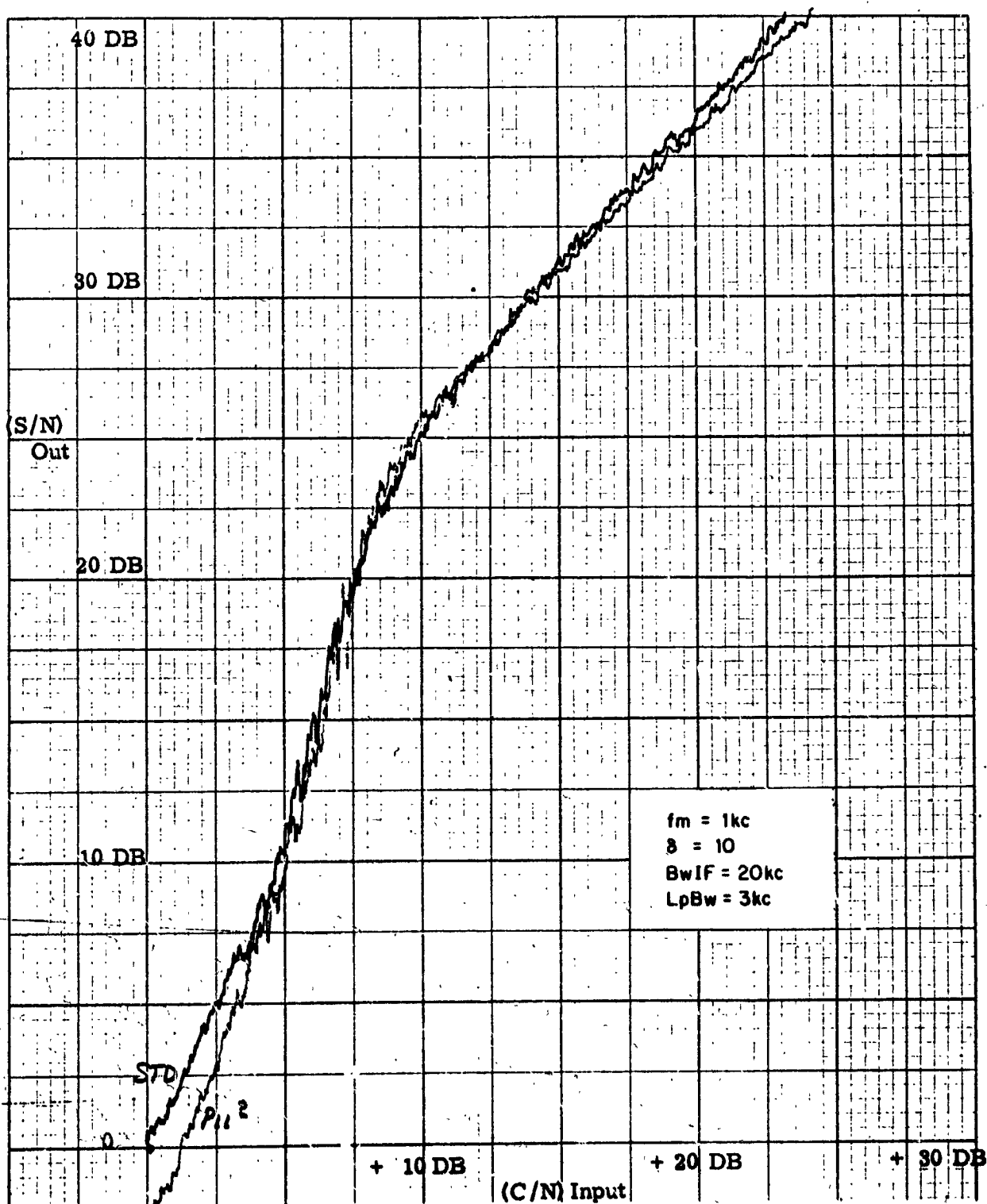


Fig. 14 Second order PLL performance for $\delta = 10$.

variation of B_{if} with the index δ may be approximated as linear for distortion measures of 1-10% and indices $\delta > 1$ so that for very large indices the $\delta^{1/2}$ dependence of B_n yields a narrower bandwidth than B_{if} and the threshold of Eq. (4.7) is lower than that of Eq. (4.8). As the index is reduced, this effect disappears and at certain indices no improvement exists. It should be finally noted that improvement at lower indices can be obtained if the B_n dependence were $\delta^{1/k}$ where $k > 2$ (as long as the proportionality coefficients are reasonably similar), and this represents the motivation for third and higher order loops.

V. HIGHER ORDER PLL DESIGN

The present section summarizes the logical design of the third order loops being synthesized at ADCOM.

5.1 The Third Order PLL

An approach similar to that of a second order PLL can be used in the logical design of the LPF for a third order loop in the presence of sinusoidal modulation. This filter is characterized by

$$F(s) = \frac{1 + \tau_1 s + (\tau_3 s)^2}{1 + \tau_2 s + (\tau_4 s)^2} = \frac{1 + \frac{s}{aB_n} + \frac{s^2}{bB_n^2}}{1 + \tau_2 s + \frac{Ks^3}{cB_n^3}} \quad (5.1)$$

where $\frac{K}{B_n} \gg a$, $\frac{K}{B_n^2} \gg b\tau_2$, and

$$a + 2 = \frac{2ab}{c} + \frac{c}{b} + \frac{b}{a} \quad (5.2)$$

and the interest is to choose K , B_n , τ_2 and any two of the three parameters (a, b, c) , the other one being defined by Eq. (5.2). The optimization is much more complicated than for the second order loop and it was shown in the First Quarterly Report to yield

$$B_n = \left(\frac{7\delta}{c\phi_c} \right)^{1/3} \omega_m \text{ cps} \quad (5.3)$$

under the conditions listed above and

$$K \gg 2c B_n \left(\frac{B_n}{\omega_m} \right)^2 \quad (5.4)$$

$$\frac{K^2}{1 + (\tau_2 \omega_m)^2} \gg c^2 B_n^2 \left(\frac{B_n}{\omega_m} \right)^4 \quad (5.5)$$

$$\left(\frac{B_n}{\omega_m}\right)^2 \gg b - 2a^2 \quad (5.6)$$

$$\left(\frac{B_n}{\omega_m}\right)^4 \gg ac - 2b^2 \quad (5.7)$$

$$\left(\frac{B_n}{\omega_m}\right)^6 \gg \frac{1}{c} \quad (5.8)$$

In order to meet these conditions and still yield a reasonably large value of c so as to get a small noise bandwidth in (5.3), the following two cases yielded a promising design for $\phi_c = \pi/2$, $\omega_m = 2\pi \times 10^3$ rad/sec:

Case I: $a = 0.3$, $b = 0.18$, $c = 0.216$

δ	B_n	$K \gg$	τ_1	τ_2	τ_3	τ_4
10	37 kc	0.5×10^6	9×10^{-5}	$\sqrt{2} \tau_4$	$\tau_1/\sqrt{2}$	$3.02\sqrt{K} \times 10^{-7}$
20	46.7 kc	10^6	7.15×10^{-5}	$\sqrt{2} \tau_4$	$\tau_1/\sqrt{2}$	$2.13\sqrt{K} \times 10^{-7}$
30	53.4 kc	1.6×10^6	6.25×10^{-5}	$\sqrt{2} \tau_4$	$\tau_1/\sqrt{2}$	$1.75\sqrt{K} \times 10^{-7}$

Case II: $a = 10$, $b = 5$, $c = 10$

δ	B_n	K	τ_1	τ_2	τ_3	τ_4
10	10.2 kc	10^7	9.77×10^{-6}	10^{-4}	4.36×10^{-5}	9.63×10^{-4}
20	12.9 kc	10^7	7.76×10^{-6}	10^{-4}	3.47×10^{-5}	6.85×10^{-4}
30	14.8 kc	10^7	6.78×10^{-6}	10^{-4}	3.15×10^{-5}	5.8×10^{-4}

Both of these cases result in complex zeroes and poles for $F(s)$ in Eq. (5.1) so that an RC passive realization is not possible. The feasibility of either a passive RC or an RLC realization are presently under consideration. The passive RC realization is a special case of the more general one described in the next section.

5.2 The Optimum Realizable PLL: Case of a Rectangular Spectrum

The optimum realizable PLL for the case where the message spectrum is given by

$$S_m(\omega) = \begin{cases} \pi/2 & , \quad |\omega| < \alpha \\ 0 & , \quad |\omega| > \alpha \end{cases} \quad (5.9)$$

was derived in the First Quarterly Report and its performance was evaluated. A series of approximations to the optimum loop were considered. These approximations are specified by

$$|1 - H(j\omega)|^2 = \frac{\left(\frac{\omega}{\beta}\right)^{2n} + \frac{1}{1 + \Lambda \delta^2}}{1 + \left(\frac{\omega}{\beta}\right)^{2n}} \quad (5.10)$$

where $H(s)$ is the closed loop transfer function, Λ is the intrinsic SNR, δ is the modulation index and β is a parameter chosen to optimize performance for a particular n . The performance evaluation previously mentioned shows that $n=3$ yields about $1\frac{1}{2}$ db of threshold improvement over an optimized second order loop at $\delta = 10$. The necessary calculations to proceed from Eq. (5.10) to a piece of hardware are now discussed.

5.2.1 Determination of the Closed Loop Transfer Function

We first rewrite Eq.(5.10) in the form

$$|1 - H(j\omega)|^2 = [1 - H(j\omega)][1 - H(-j\omega)] = \frac{1 + \left(\frac{\omega}{\beta}\right)^6}{(1 + \Lambda \delta^2) \left[1 + \left(\frac{\omega}{\beta}\right)^6\right]} \quad (5.11)$$

where

$$\beta' = \frac{\beta}{(1 + \Lambda \delta^2)^{1/6}}$$

Next we note that the factors of $1 + x^6$ are given by

$$(1 + jx)(1 - jx)(1 + jx - x^2)(1 - jx - x^2)$$

and assigning all singularities in the RHS of the complex plane to $1 - H(-j\omega)$ and the remainder ones to $1 - H(j\omega)$, we find

$$1 - H(j\omega) = \frac{1}{\sqrt{1 + \Lambda\delta^2}} \cdot \frac{[1 + j(\frac{\omega}{\beta'})][1 + j(\frac{\omega}{\beta'}) - (\frac{\omega}{\beta'})^2]}{[1 + j(\frac{\omega}{\beta})][1 + j(\frac{\omega}{\beta}) - (\frac{\omega}{\beta})^2]} \quad (5.12)$$

Transposing and using the expression for β' we have

$$H(j\omega) = \frac{\sqrt{1 + \Lambda\delta^2} - 1 + 2j[\sqrt{1 + \Lambda\delta^2} - 6\sqrt{1 + \Lambda\delta^2}](\frac{\omega}{\beta}) - 2[\sqrt{1 + \Lambda\delta^2} - 3\sqrt{1 + \Lambda\delta^2}](\frac{\omega}{\beta})^2}{\sqrt{1 + \Lambda\delta^2} [1 + j(\frac{\omega}{\beta})][1 + j(\frac{\omega}{\beta}) - (\frac{\omega}{\beta})^2]} \quad (5.13)$$

Now we have determined the closed loop transfer function except for the parameter β which should be chosen so as to minimize the mean square loop error σ^2 . The contribution to loop error due to distortion is given by

$$\text{Var}[e_{ld}(t)] = \frac{\delta^2}{\alpha} \int_0^{\infty} |1 - H(j\omega)|^2 d\omega \quad (5.14)$$

which for Eq.(5.10) yields

$$\text{Var}[e_{ld}(t)] = \frac{\delta^2}{7} \left(\frac{\alpha}{\beta}\right)^6 \quad (5.15)$$

for $(\frac{\alpha}{\beta})^3 \ll 13/7$ and $\Lambda\delta^2 \gg 1$, where the first condition is always met for Eq. (5.15) less than unity and the second condition is also satisfied for above-threshold performance.

Meanwhile, the contribution to loop error due to noise error is given by

$$\text{Var}[e_{ln}(t)] = \frac{2}{\pi\Lambda\alpha} \int_0^{\infty} |H(j\omega)|^2 d\omega \quad (5.16)$$

From Eq.(5.13) we find that

$$|H(j\omega)|^2 = \frac{[\sqrt{1+\Lambda\delta^2} - 1 - 2(\sqrt{1+\Lambda\delta^2} - 3\sqrt{1+\Lambda\delta^2})(\frac{\omega}{\beta})^2]^2 + 4[\sqrt{1+\Lambda\delta^2} - 6\sqrt{1+\Lambda\delta^2}](\frac{\omega}{\beta})^2}{(1 - \Lambda\delta^2)[1 + (\frac{\omega}{\beta})^6]} \quad (5.17)$$

so that inserting Eq. (5.17) into Eq. (5.16) we find that

$$\text{Var}[e_{\ell n}(t)] = \frac{\pi(\beta/\alpha)}{3\Lambda(1+\Lambda\delta^2)} [5(1+\Lambda\delta^2) - 6(1+\Lambda\delta^2)^{5/6} + 1] \quad (5.18)$$

If we now define a parameter $X(\Lambda\delta^2)$ as

$$X(\Lambda\delta^2) = \frac{\pi}{3(1+\Lambda\delta^2)} [5(1+\Lambda\delta^2) - 6(1+\Lambda\delta^2)^{5/6} + 1] \quad (5.19)$$

we can rewrite Eq. (5.18) as

$$\text{Var}[e_{\ell n}(t)] = \frac{X(\Lambda\delta^2)}{\Lambda} \left(\frac{\beta}{\alpha}\right) \quad (5.20)$$

The total mean square error is given by the sum of Eqs.

(5.15) and (5.20):

$$\sigma^2 = \frac{\delta^2}{7} \left(\frac{\beta}{\alpha}\right)^{-6} + \frac{X}{\Lambda} \left(\frac{\beta}{\alpha}\right) \quad (5.21)$$

so that differentiating this with respect to $(\frac{\beta}{\alpha})$ and setting the result equal to zero, we find that the minimum occurs for

$$\left(\frac{\beta}{\alpha}\right) = \left(\frac{6}{7} \frac{\Lambda\delta^2}{X}\right)^{1/7} \quad (5.22)$$

and substitution of this into Eq. (5.21) gives

$$\sigma^2 = \left(\frac{7}{6} X\right)^{6/7} \left(\frac{\delta}{\Lambda^3}\right)^{2/7} \quad (5.23)$$

A proper choice for the threshold is $\sigma^2 = \frac{1}{4}(\text{rad})^2$. Substitution of this value into Eq. (5.23) gives the equation of the threshold curve of the optimized demodulator as

$$\delta = 4.95 \times 10^{-3} \left(\frac{\Lambda}{X} \right)^3 \quad (5.24)$$

If X were a simple function of $\Lambda\delta^2$ we could plot the threshold curve immediately. The simplest method in the present situation is to use the following procedure:

- Assume a value of $\Lambda\delta^2$, say k , and draw the straight line (plotting δ versus Λ in logarithmic co-ordinates) corresponding to $\Lambda\delta^2 = k$.
- Use the definition of $X(\Lambda\delta^2)$ given by Eq. (5.19) to calculate $X(k)$. Then draw the straight line corresponding to Eq. (5.24) with $X(\Lambda\delta^2) = X(k)$.
- The intersection of the straight lines drawn in (a) and (b) is a point on the desired threshold curve. The procedure may be repeated with different values of k to give the complete curve.

This procedure has been carried out to give the threshold curve in Fig. 15.

From Fig. 15 we can read the values of intrinsic signal-to-noise ratio (Λ) at threshold for loops operating at any desired modulation indices, the values for 10, 20 and 30 listed in Table I. The values of Λ and δ may be inserted into Eq. (5.19) to calculate the corresponding value of X ; this in turn can be used to calculate (β/α) from Eq. (5.22). These values, which are necessary in determining the transfer function to be synthesized, are also listed in Table I.

Table I
LOOP PARAMETERS AT THRESHOLD

δ	10	20	30
Λ	16.7 db	18.1 db	18.9 db
(β/α)	2.71	3.42	3.91

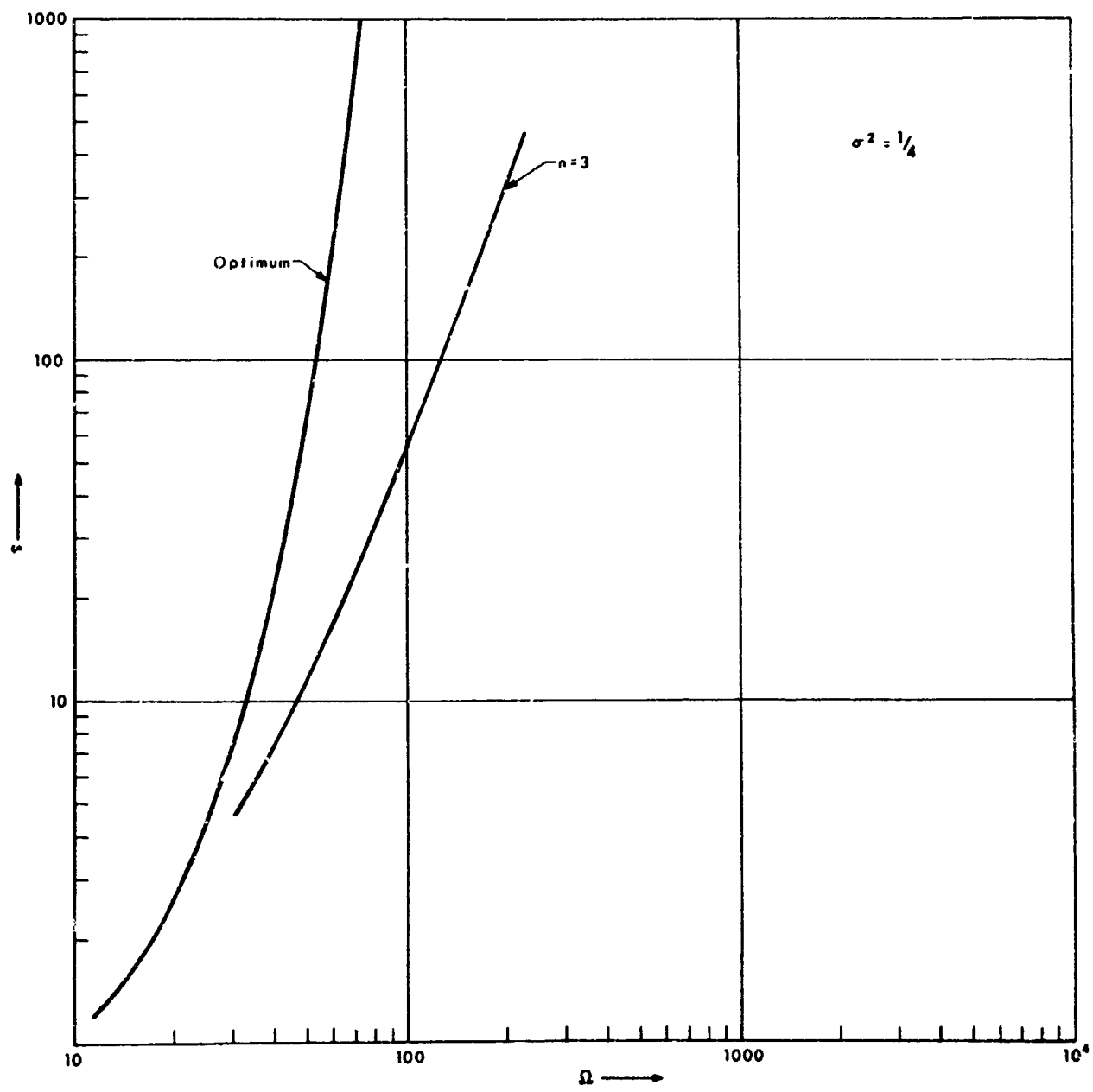


Fig. 15 Threshold curve for third order loop filters.

5.2.2 Determination of the Open Loop Transfer Function

In the preceding section we determined the closed loop transfer function $H(j\omega)$ in terms of Λ , δ , and (β/α) . We wish to build systems which are optimum at threshold for a given modulation index. The values of Λ , δ , and (β/α) listed in Table I are appropriate for these requirements. Therefore, by inserting a set of these values into Eq. (5.13) (and using $\alpha = 2\pi \cdot 1000$ cps as the experimental modulation frequency) we obtain a numerical expression for the closed-loop transfer function which we wish to synthesize. However, since we will be synthesizing only the loop filter transfer given by

$$F(s) = \frac{sH(s)}{K[1 - H(s)]} \quad (5.25)$$

so that for the $H(s)$ given by Eq. (5.13)

$$F(s) = \frac{s}{K} \frac{\sqrt{1 + \Lambda\delta^2} - 1 + 2(\sqrt{1 + \Lambda\delta^2} - \sqrt[6]{1 + \Lambda\delta^2})(\frac{s}{\beta}) + 2(\sqrt{1 + \Lambda\delta^2} - \sqrt[3]{1 + \Lambda\delta^2})(\frac{s}{\beta})^2}{[1 + \sqrt[6]{1 + \Lambda\delta^2}(\frac{s}{\beta})][1 + \sqrt[6]{1 + \Lambda\delta^2}(\frac{s}{\beta}) + \sqrt[3]{1 + \Lambda\delta^2}(\frac{s}{\beta})^2]} \quad (5.26)$$

We can write this in a more compact form by defining some new time constants as

$$F(s) = A_o \frac{A'}{A} \frac{sT_3'}{1 + sT_1' + s^2T_1'T_2'} \cdot \frac{1 + sT_1 + s^2T_1T_2}{1 + sT_3} \quad (5.27)$$

As it stands, $F(s)$ does not provide a d-c path. This will be necessary to keep the center frequency of the VCO from drifting away from the carrier frequency. For this reason we modify $F(s)$ to include a d-c path: as

$$F(s) = A_o \frac{A'}{A} \frac{1 + sT_3'}{1 + sT_1' + s^2T_1'T_2'} \cdot \frac{1 + sT_1 + s^2T_1T_2}{1 + sT_3} \quad (5.28)$$

With this definition of the time constants we have the following equivalences:

$$KA_o T_3' \frac{A'}{A} = \sqrt{1 + \Lambda \delta^2} - 1 = \text{Total loop gain} \quad (5.29)$$

$$T_1 = \frac{2}{\beta} \frac{\sqrt{1 + \Lambda \delta^2} - \sqrt[6]{1 + \Lambda \delta^2}}{\sqrt{1 + \Lambda \delta^2} - 1} \quad (5.30)$$

$$T_2 = \frac{1}{\beta} \frac{\sqrt{1 + \Lambda \delta^2} - \sqrt[3]{1 + \Lambda \delta^2}}{\sqrt{1 + \Lambda \delta^2} - \sqrt[6]{1 + \Lambda \delta^2}} \quad (5.31)$$

$$T_3 = T_1' = T_2' = \frac{1}{\beta} \sqrt[6]{1 + \Lambda \delta^2} \quad (5.32)$$

$T_3' =$ (we must choose this so that $sT_3' \gg 1$ except at frequencies near d-c)

Using the values of Λ , δ , and (β/α) from Table I we may calculate the values of the time constants shown in Table II.

Table II

TIME CONSTANT VALUES

δ	10	20	30
$KA_o T_3' \frac{A'}{A}$	67.5	160.1	262
T_1	1.121×10^{-4}	9.03×10^{-5}	8.00×10^{-5}
T_2	4.72×10^{-5}	3.93×10^{-5}	3.53×10^{-5}
T_3	2.41×10^{-4}	2.53×10^{-4}	2.62×10^{-4}
T_1'	2.41×10^{-4}	2.53×10^{-4}	2.62×10^{-4}
T_2'	2.41×10^{-4}	2.53×10^{-4}	2.62×10^{-4}
T_3'	1.00×10^{-2}	1.00×10^{-2}	1.00×10^{-2}

The problem of synthesizing a network having the transfer function of Eq. (5.28) may be approached in many different ways. The approach chosen here is to design an active network including an operational amplifier. With the arrangement shown in Fig. 16, the overall transfer function is given by

$$F(s) = A_o \frac{Z'(s)}{Z(s)} \quad A_{op} \gg 1 \quad (5.33)$$

This will be identical to Eq. (5.28) if we let

$$Z'(s) = A' \frac{1 + sT_3}{1 + sT_1 + s^2 T_1 T_2} \quad (5.34)$$

and

$$Z(s) = A \frac{1 + sT_3}{1 + sT_1 + s^2 T_1 T_2} \quad (5.35)$$

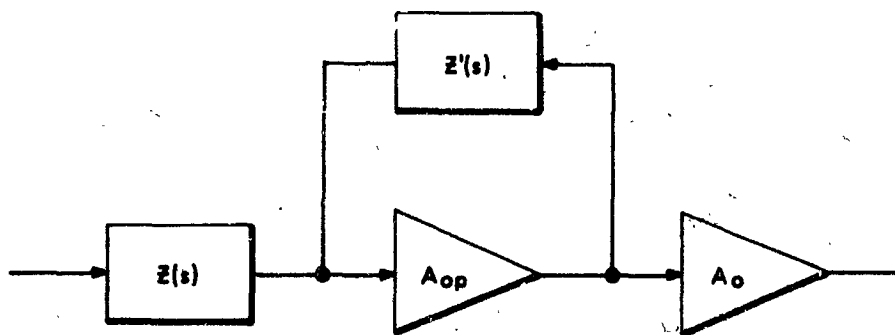


Fig. 16 Configuration of active filter network.

To synthesize the impedance $Z(s)$ we choose the circuit configuration shown in Fig. 17a. (We must use a configuration which allows complex poles.) For this circuit, the following relations hold*

$$R_1 = \frac{A}{2} \quad (5.36)$$

$$R_2 = \frac{AT_1(T_3 - T_2)}{4[T_3^2 - T_1(T_3 - T_2)]} \quad (5.37)$$

$$C_1 = \frac{4[T_3^2 - T_1(T_3 - T_2)]}{AT_3} \quad (5.38)$$

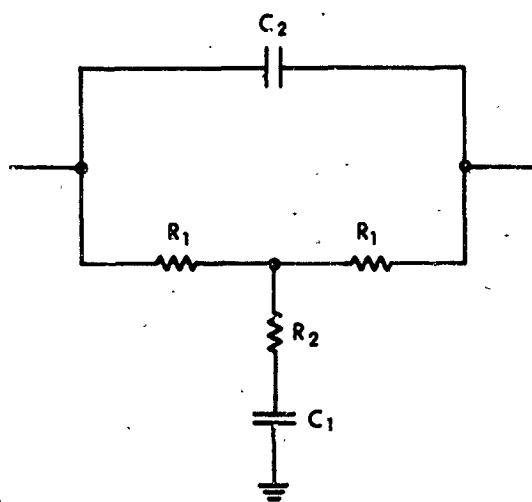
$$C_2 = \frac{T_1 T_2}{AT_3} \quad (5.39)$$

Using these equations and the values of the time constants, T_1, T_2, T_3 given in Table II we can calculate the component values suitable for the different modulation indices and these are tabulated in Table III.

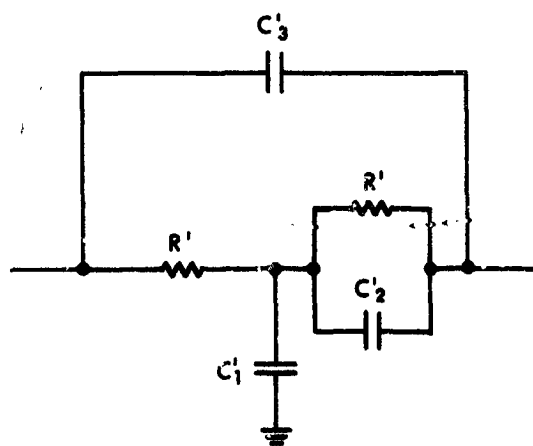
Table III
COMPONENT VALUES FOR $Z(s)$

	$\delta = 10$	$\delta = 20$	$\delta = 30$
R_1	0.5A	0.5A	0.5A
R_2	0.150A	0.1081A	.0899A
C_1	$\frac{6.03 \times 10^{-4}}{A}$	$\frac{7.07 \times 10^{-4}}{A}$	$\frac{7.71 \times 10^{-4}}{A}$
C_2	$\frac{2.20 \times 10^{-5}}{A}$	$\frac{1.402 \times 10^{-5}}{A}$	$\frac{1.078 \times 10^{-5}}{A}$

* Landee, Davis, and Albrecht, "Electronic Designers' Handbook," McGraw-Hill, New York, 1957.



a Circuit of $Z(s)$



b Circuit of $Z(s)$

Fig. 17 Circuits for synthesizing impedances.

The parameter A may be chosen so that these component values are of reasonable magnitude.

To synthesize the impedance $Z'(s)$ we choose a different circuit configuration (Fig. 17b) which gives more reasonable component values in spite of the large value of T'_3 . With this circuit we have the following relationships:

$$R' = \frac{A'}{2} \quad (5.40)$$

$$C'_1 = \frac{2[2T_3'^2 - T_1'(T_3' - T_2')]}{A'T_3'} \quad (5.41)$$

$$C'_2 = \frac{2T_1'(T_3' - T_2')}{A'T_3'} \quad (5.42)$$

$$C'_3 = \frac{T_1'T_2'}{A'T_3'} \quad (5.43)$$

Substitution of the time constants from Table II into these equations gives the component values listed in Table IV. The parameter A' may be chosen so that these component values are of reasonable magnitude.

Table IV
COMPONENT VALUES FOR $Z'(s)$

	$\delta = 10$	$\delta = 20$	$\delta = 30$
R'_1	$0.5A'$	$0.5A'$	$0.5A'$
C'_1	$\frac{3.95 \times 10^{-2}}{A'}$	$\frac{3.95 \times 10^{-2}}{A'}$	$\frac{3.95 \times 10^{-2}}{A'}$
C'_2	$\frac{4.70 \times 10^{-4}}{A'}$	$\frac{4.94 \times 10^{-4}}{A'}$	$\frac{5.10 \times 10^{-4}}{A'}$
C'_3	$\frac{5.81 \times 10^{-6}}{A'}$	$\frac{6.40 \times 10^{-6}}{A'}$	$\frac{6.86 \times 10^{-6}}{A'}$

One final observation based on Table II is that the only loop parameter which is strongly dependent on the modulation index δ is the loop gain. This suggests the possibility of designing a loop which will operate well at different modulation indices with adjustment of the loop gain only.

VI. OUTLINE OF WORK PLANS

The work plans for the next interval are briefly outlined in this section.

6.1 Theoretical Work

- a) Study of the band-dividing analysis presented by S. Darlington in his B.S. T. J. paper.
- b) Study of the possibility of using Bode filters in the PLL demodulator.
- c) Study of non-sinusoidal phase detector characteristics that could be used to provide a threshold reduction in the PLL demodulator.
- d) Study of threshold combating techniques based on the suppression or attenuation of the effects of the "impulses" that occur near threshold in FM demodulators.

6.2 Experimental Work

- a) Completion of the second order loop threshold tests.
- b) Synthesis of the third order loop filters followed by the corresponding third order loop tests.
- c) Experimental study of the threshold performance of an FCF (frequency-compressive feedback) system existing at ADCOM and designed for FM threshold reduction.
- d) Implementation of promising non-sinusoidal phase detectors and threshold combating techniques in accordance to the results of the theoretical study.